MOL.20000209.0233

OFFICE OF CIVILIAN RADIOACTIVE WASTE MANAGEMENT
CALCULATION COVER SHEET

1. QA: QA

Page: 1 Of: 42

2. Calculation Title
Intact and Degraded Criticality Calculations for the Codisposal of Shippingport PWR Fuel in a Waste Package

3. Document Identifier (including Revision Number)
CAL-EDC-NU-000002 REV 00

MOL.20000209.0233

4. Total Attachments	5. Attachment Numbers - Number of pages in each
4	I-2, II-3, III-2, IV-5

	Print Name	Signature	Date
6. Originator	Soon Sam Kim	Soon Sam Kim	12/21/99
7. Checker	Horia R. Radulescu	Horia R. Radulescu	12/21/99
8. Lead	J. Wesley Davis	Hugh A. Benton for J. WESLEY DAVIS	12/22/99

9. Remarks

Revision History

10. Revision No.	11. Description of Revision
00	Initial Issue

CONTENTS

Page

CONTENTS (Continued)

Page

FIGURES

Page

TABLES

Page

1. PURPOSE

The purpose of this calculation is to characterize the criticality safety concerns for the codisposal of Shippingport pressurized water reactor (SP PWR) spent nuclear fuel (SNF) contained in a standardized Department of Energy (DOE) SNF canister, and high-level waste (HLW) glass in a waste package (WP) placed in a Monitored Geologic Repository (MGR). The result of this calculation will be used to evaluate criticality issues and provide input for the DOE SNF canister design, referred to as "the canister" in this document.

This document has been prepared in accordance with Procedure AP-3.12Q, Revision 0, ICN 0, Calculations.

2. METHOD

The calculation method employs the use of MCNP Version 4B2 computer code (Ref. 1) to calculate the effective neutron multiplication factor (k_{eff}) for various geometrical configurations of SP PWR SNF.

3. ASSUMPTIONS

3.1 Beginning of Life (BOL) pre-irradiation fuel composition is used for all calculations for intact fuel cluster. The basis of this assumption is that it is conservative to assume unirradiated fuel since it is more neutronically reactive than spent fuel. This assumption is used in Section 5.2.1.

3.2 The fuel subcluster represented was 8.719312-cm (3.4328-in.) square, with active fuel length of 246.38 cm (97.0 in.) and plate length of 248.02592 cm (97.648 in.). Other structural materials were neglected. Note that the extra digits shown in metric units in this report are the result of conversion from English units and do not represent enhanced accuracy. The basis of this assumption is that it is conservative to neglect structural materials because they provide some additional amount of neutron absorption. This assumption is used throughout Section 5.

3.3 Burnable neutron absorber material in two end plates (referred to as "poison wafers" in Figure 5-4) of the fuel subcluster (eight end plates per cluster) were represented as water. The basis of this assumption is that it is conservative to neglect the burnable neutron absorber material since it provides some additional amount of neutron absorption. This assumption is used for all calculations in Section 5.2.1 and Sections 5.2.2.1 through 5.2.2.3.

3.4 The curved bottom and top carbon steel impact plates of the canister were represented as the 2-in. carbon steel slab. The ends of the canister were simplified and represented as "squared off." The basis of this assumption is that it is conservative to neglect this portion of the canister since it provides a small amount of neutron absorption. This assumption is used in Section 5.1.2.

3.5 At least 30 cm of full-density water (1.0 g/cm^3) surrounding the WP was used in all cases to represent neutron reflector. This is based on a 30-cm thick water reflection being effectively equivalent to an infinite neutron reflector (Ref. 2, p. 107). This assumption is used throughout Section 5.

3.6 For degradation analysis, stainless steel degrades to goethite, FeOOH, and all other constituents of the steel are neglected and represented as water in the calculations. The basis of this assumption is that it is conservative to neglect the non-iron components of the stainless steel since they provide some small amount of neutron absorption. This assumption is used throughout Section 5.2.

3.7 For some cases where goethite or clayey materials accumulate at the bottom of the canister or the WP, the coolant channel and the cruciform areas of the fuel cluster were assumed to be filled with water. The basis of this assumption is that as shown in Sections 6.1.3 and 6.2.2, it is more reactive with water instead of goethite or clay mixture in those areas. This assumption is used throughout Section 5.2.

3.8 Pu, U, and B isotopes in the postbreach clayey material were neglected in the calculations. The basis of the assumption is that their contents does not affect the k_{eff}. This assumption is used in Section 5.1.5.

3.9 B, Gd, and Li isotopes in the J-13 well water composition were neglected in the calculations because their contents are insignificant. The basis of this assumption is that it is conservative because these isotopes provide some additional amount of neutron absorption. This assumption is used in Section 5.1.5.

3.10 Aluminum cross section is used instead of zinc cross section in the MCNP input since the cross section of zinc is not available in either ENDF/B-V or ENDF-VI cross-section libraries. The basis of this assumption is that it is conservative since the thermal-neutron capture cross section and the resonance integral of zinc (1.1 and 2.8 barn, respectively, Ref. 16) are greater than those of aluminum (0.23 and 0.17 barn, respectively, Ref. 16). This assumption is used throughout Section 5.

3.11 Ba-138 cross section is used instead of Ba-137 cross section in the MCNP input since the cross section of Ba-137 is not available in either ENDF/B-V or ENDF-VI cross-section libraries. The basis of this assumption is that it is conservative since the thermal-neutron capture cross section and the resonance integral of Ba-137 (5.1 and 4 barn, respectively, Ref. 16) are greater than those of Ba-138 (0.45 and 0.3 barn, respectively, Ref. 16). This assumption is used throughout Section 5.

4. USE OF COMPUTER SOFTWARE AND MODELS

4.1 SOFTWARE APPROVED FOR QUALITY ASSURANCE (QA) WORK

4.1.1 MCNP4B2

MCNP4B2 computer code is used to calculate the effective neutron multiplication factor (k_{eff}) for nuclear criticality evaluations (Ref. 4).

- Program Name: MCNP
- Version/Revision Number: Version 4B2
- Computer Software Configuration Item (CSCI) Number: 30033 V4B2LV
- Computer Type: Hewlett Packard 9000 Workstations

Each input file used is echoed in its output file. The output files are listed in Attachment II; they are stored on electronic media (Ref. 15).

a) The MCNP4B2 computer code (Ref. 1) is an appropriate tool to be utilized to perform the criticality calculations reported in this document.
b) This software has been validated over the range it was used.
c) It was previously obtained from the Civilian Radioactive Waste Management System (CRWMS) Management and Operating Contractor (M&O) Software Configuration Management (SCM) in accordance with appropriate procedures.

4.2 SOFTWARE ROUTINES

4.2.1 Excel

- Title: Excel
- Version/Revision Number: Microsoft Excel 97

The Excel spreadsheet program was used to perform simple numeric calculations as documented in Section 5 of this calculation. The user-defined formulas, inputs, and results were documented in sufficient detail in Section 5 to allow an independent repetition of the various computations. The Excel files are stored on electronic media (Ref. 15).

4.3 MODELS

None used.

5. CALCULATION

This section describes the calculations performed to calculate k_{eff} of the codisposal WP with the canister containing intact or degraded Shippingport PWR fuel cluster. The intact codisposal WP, including the fuel cluster and the canister, is described in Section 5.1. Chemical compositions of the materials used in the calculations are summarized in Tables 5-2 through 5-9 in Section 5.1.5. Description of the MCNP calculations is given in Section 5.2. Calculations for the intact fuel cluster are described in Section 5.2.1. Calculations for the partially and the fully degraded fuel cluster are described in Section 5.2.2. MCNP output files are stored on electronic media labeled as *CD-Shippingport PWR Files* (Ref. 15). Results of the calculations are presented in Section 6.

Unqualified data are used in the calculations reported in this document. However, the unqualified data are only used to determine the bounding values for the fuel group by establishing the limits based on the representative fuel type (Shippingport PWR) for this group (HEU oxide fuel). Hence, the input values used for criticality calculations of Shippingport PWR SNF do not constitute data that have to be qualified in this application. They merely establish the bounds for acceptance. Since the input values are not relied upon directly to address safety and waste isolation issues, nor do the design inputs affect a system characteristic that is critical for satisfactory performance, according to the governing procedure (AP-3.15Q), data do not need to be controlled as TBV (to be verified).

5.1 CALCULATION INPUTS

The description of the Shippingport PWR fuel is taken from the Shippingport PWR fuel characteristics document, Ref. 5. All fuel and canister related information is from this reference unless otherwise noted. Compositions for structural and other nonfuel related materials are from Ref. 6.

The Shippingport PWR was operated with two sequential cores, Core 1 and Core 2 (C1 and C2). Core 2 had more than five times the design energy output and twice the power density of Core 1. This required the development of a fuel cluster having many desirable characteristics: high fissile loading, resistance to irradiation damage, and stability at high heat fluxes. Since uranium dioxide demonstrated these characteristics in Core 1, it was selected as the fuel matrix for Core 2. The Core 2 also included the introduction of radial fuel zoning for improved thermal capability. Core 2 had Seed 1 and Seed 2 fuel clusters. The Seed 2 cluster had a higher U-235 loading per cluster (19.5 kg U-235) than the Seed 1 cluster (16.8 kg U-235). The Core 2 Seed 2 (C2 S2) fuel cluster is represented in the criticality calculations to envelop all of the different fuel types.

Note that the extra digits shown in metric units in this report are a result of converting from English units and do not represent enhanced accuracy.

5.1.1 Description of Shippingport PWR C2 S2 Fuel Cluster

The Shippingport PWR C2 S2 fuel cluster is composed of four fuel subclusters arranged in a square array with 1.194 cm (0.47 in.) spacing between them to form a cruciform-shaped channel in the center of the fuel cluster. This channel accommodated a control rod that was inserted down the center of the cluster. The C2 S2 cluster, as shown in Figure 5-1, is 18.7452-cm (7.38-in.) square, and 265.43-cm (104.5-in.) long. A cross-sectional view of the MCNP fuel cluster representation is shown in Figure 5-2. The bottom right subcluster is oriented as in Figure 5-2. The top right subcluster is identical but rotated 90° counterclockwise. The top left subcluster is rotated 180° counterclockwise, and the bottom left subcluster is rotated 270° counterclockwise.

The C2 S2 subcluster is a 8.7376-cm (3.440-in.) square, with the active fuel length of 246.38 cm (97.0 in.). The C2 S2 subcluster contains nineteen fuels and two neutron absorber plates. The fuel plate is formed (see Figure 5-3) by sandwiching a strip of 0.09144-cm (0.036-in.)-thick enriched UO_2-ZrO_2-CaO alloy wafers between two 0.05207-cm (0.0205-in.)-thick Zircaloy-4 cover plates and four side strips. The uranium (U-235) enrichment at the beginning of life is 93.2%. The fuel meat occupies 87.5% (Ref. 3, p. 22) of the fuel wafer volume. This is production density as a percentage of theoretical density. The remaining void volume of the fuel wafer is called "wafer porosity volume." The plate void space is calculated by subtracting total fuel wafer volume from the actual fuel volume of the fuel cluster. Two end plates contain a 0.04-in.-thick neutron absorbing material. This neutron absorbing material region is represented as water. The C2 S2 subcluster has three zones of fuel wafers (see Figure 5-4) with varying compositions, as shown in Table 5-1.

Table 5-1. Fuel Wafer Compositions for the C2 S2 fuel

Zone Number	UO_2-ZrO_2-CaO	Fissile Loading (kg)
1	54.9 w/o UO_2 39.9 w/o ZrO_2 5.2 w/o CaO	7.076
2	40.2 w/o UO_2 54.0 w/o ZrO_2 5.8 w/o CaO	8.987
3	26.5 w/o UO_2 67.1 w/o ZrO_2 6.4 w/o CaO	3.437
Total BOL/Cluster		19.500

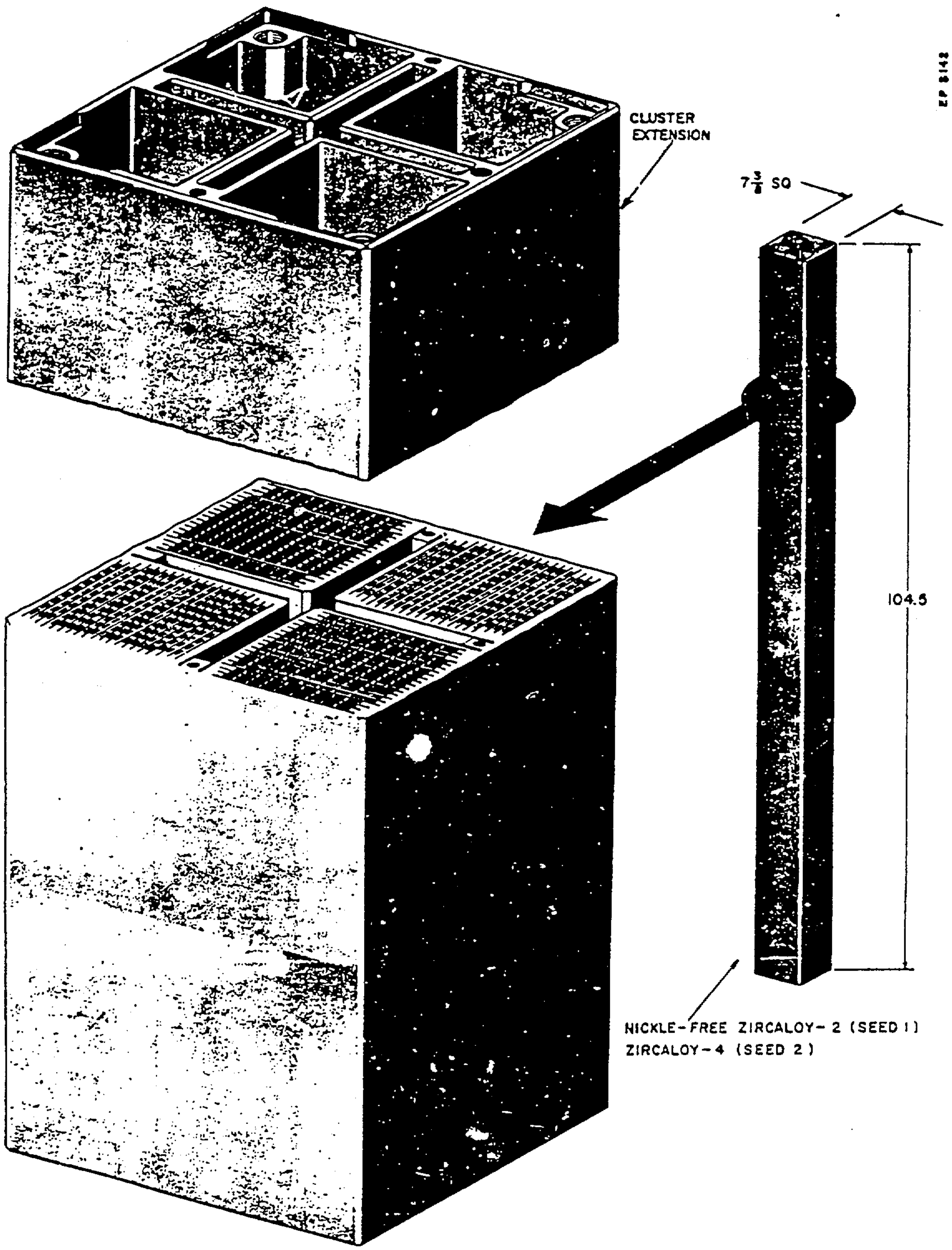

Figure 5-1. Seed Fuel Cluster with Cruciform Control Rod Channel

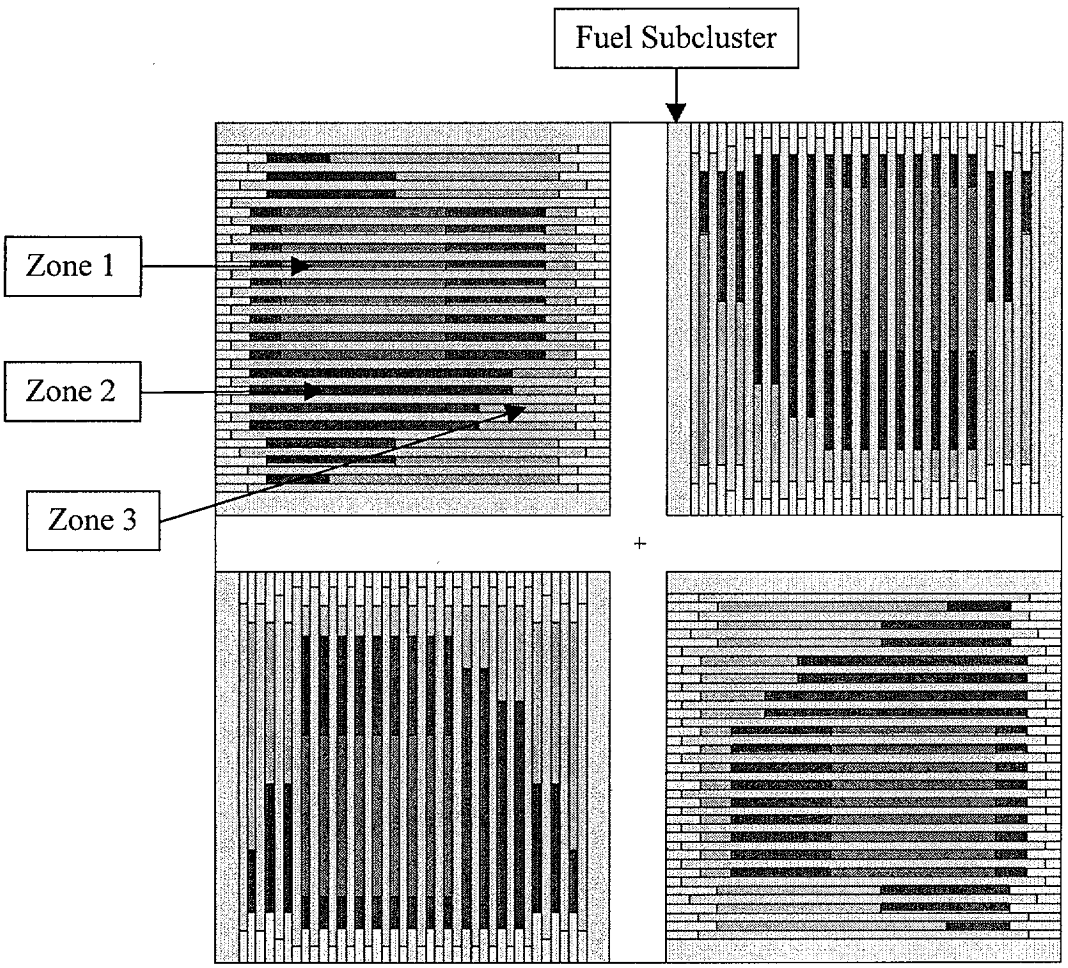

Figure 5-2. Cross-Sectional View of the MCNP Fuel Cluster Representation

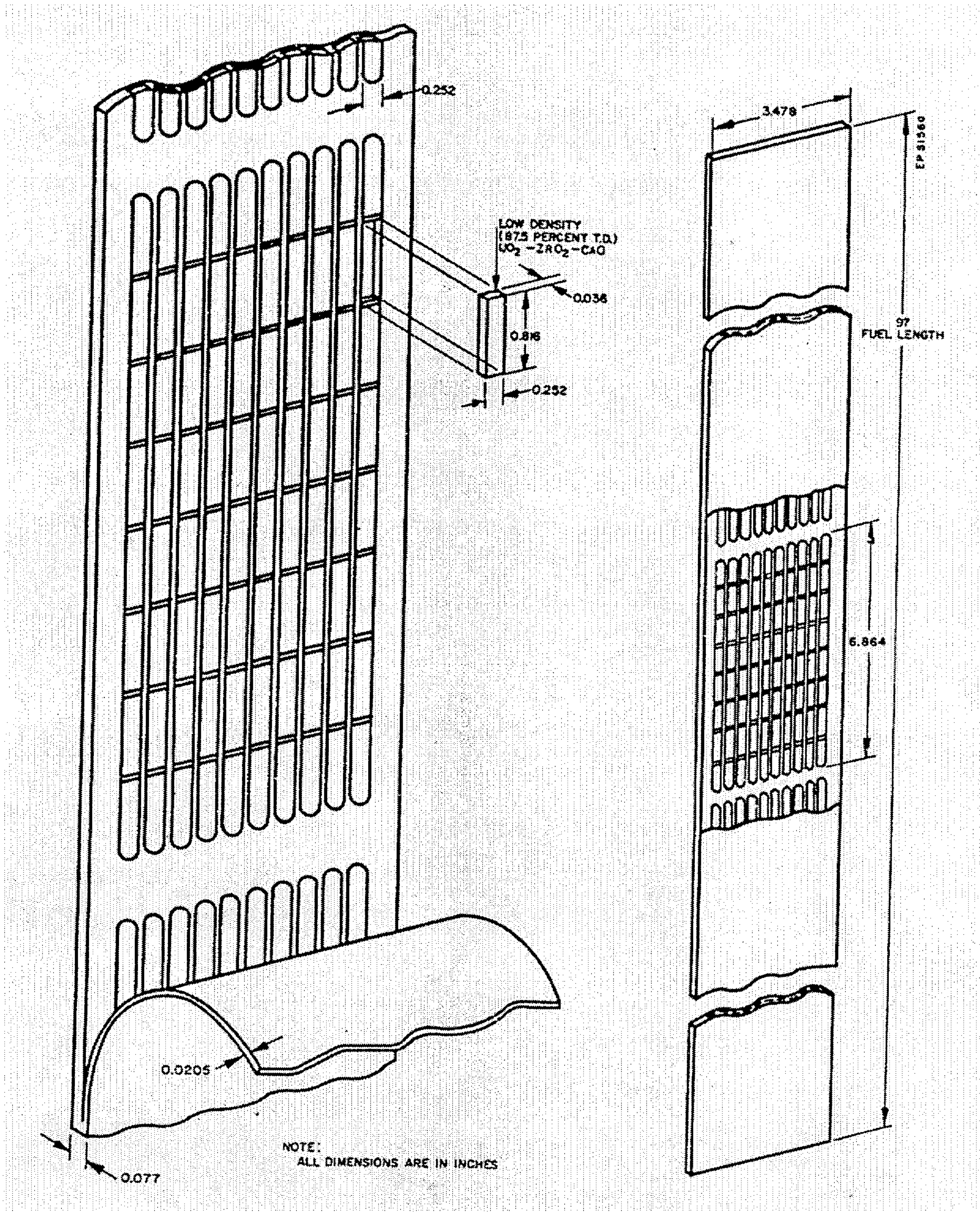

Figure 5-3. Seed Cross Section Showing Fuel Wafer Compartment

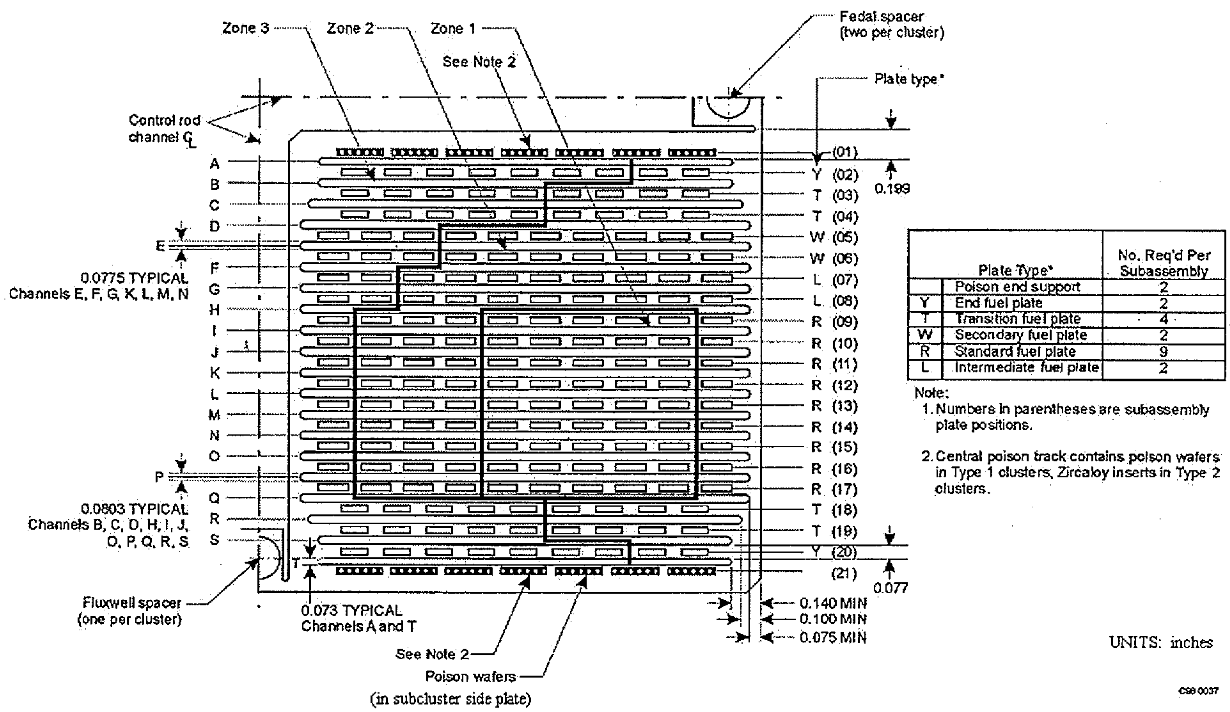

Figure 5-4. Shippingport PWR Core 2 Seed 2 Subcluster Cross Section

5.1.2 Description of Canister

The description of the canister is taken from Ref. 7. The canister is a right circular cylinder of stainless steel (Type 316L). The outside diameter of the canister is 457.2 mm (18 in.) with a wall thickness of 9.5 mm (0.374 in.). The canister is also referred to as the 18-in. canister. The nominal internal length of the canister reserved for fuel loading is 268.09 cm (105.547 in.). The base plate is 19-mm (0.748-in.) thick, and the top spacer plate is 9.5-mm (0.374-in.) thick. The nominal internal length of the empty space above the top spacer plate to the impact plate is 140.75 cm (55.413 in.). The inner radius of the spacer cylinder in the empty space is 20.615 cm (8.116 in.) and 0.635-cm (0.25-in.) thick. A detailed sketch of the canister is shown in Attachment I. The canister also contains 9.5-mm (0.374-in.)-thick stainless steel (Type 316L) guide plates (A-Guide) that are used to hold the Shippingport PWR SNF cluster. The guide plates are not a standard part of the 18-in. canister, but are designed specific to the SNF to be inserted into the canister. The guide plates are designed such that the center position can hold one Shippingport PWR SNF cluster. Figure 5-5 shows the cross-sectional view of the MCNP case representing the canister loaded with a single fuel cluster.

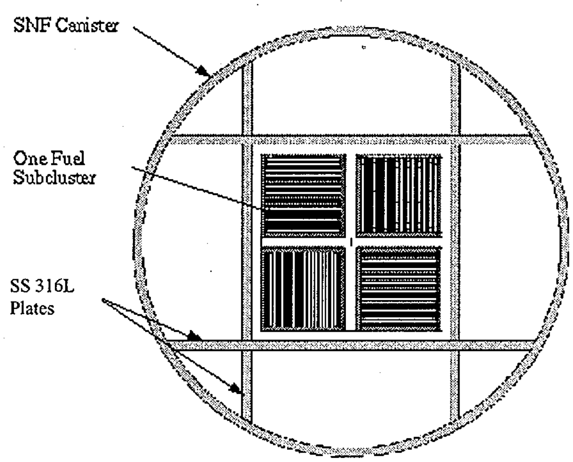

Figure 5-5. Cross-Sectional View of the Canister

5.1.3 Codisposal WP

The codisposal WP contains five HLW glass pour canisters surrounding an 18-in. canister (see Figure 5-6). The WP barrier materials are typical of those used for commercial SNF WPs. The inner barrier is composed of a 20-mm (0.7874-in.)-thick Alloy 22 and serves as a corrosion resistant material. The outer barrier is composed of a 100-mm-thick carbon steel (ASTM A 516 Grade 70) and serves as a corrosion allowance material. The outside diameter of the WP is 2120 mm (83.465 in.) and inside cavity length is 4617 mm (181.772 in.). The inner barrier lids are 25-mm (0.984-in.) thick and the outer barrier lids are 110-mm (4.33-in.)-thick. There is a 30-mm

(1.181-in.) closure lid gap between the upper inner and outer barrier lids. There is a 225-mm (8.858-in.)-long skirt at each end of the codisposal WP.

The canister is placed in a 31.75-mm (1.25-in.)-thick carbon steel (ASTM A 516 Grade 70) support tube with a 565-mm (22.244-in.) nominal outer diameter. The support tube is connected to the inside wall of the codisposal WP by web-like carbon steel (ASTM A 516 Grade 70) plates that form emplacement positions for the HLW glass pour canisters equally spaced about the center support tube. The support tube and plates are 4597-mm (180.984-in.) long.

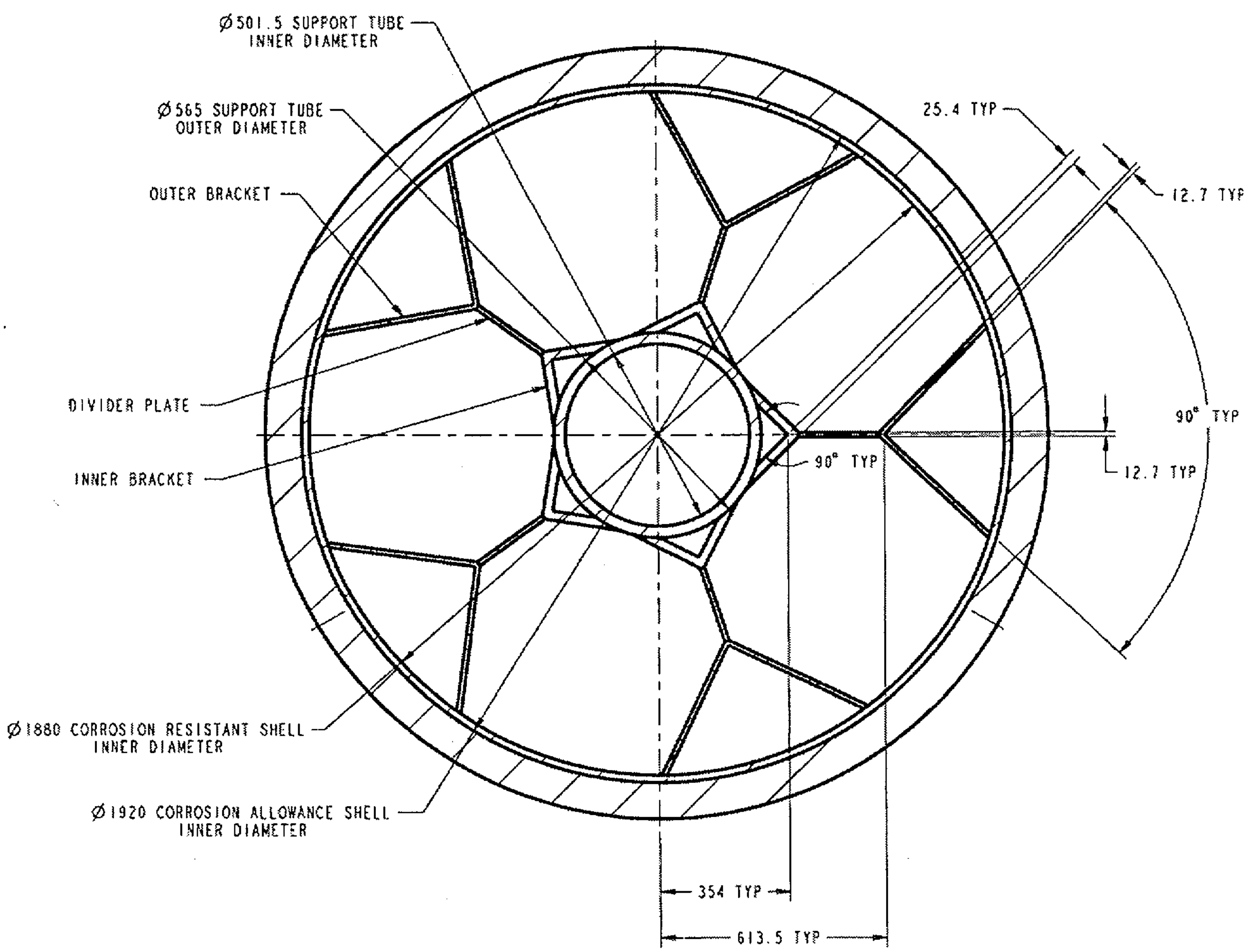

NOTE: TYP = typical

Figure 5-6. 5-HLW/DOE Spent Fuel-Long Codisposal WP

5.1.4 HLW Glass Pour Canisters

The Hanford 15-foot HLW glass pour canister is a cylindrical stainless steel (Type 304L) shell with an outer diameter of approximately 610 mm (24.00 in.), a wall thickness of 10.5 mm (0.413 in.), and a nominal length of 4572 mm (180 in.). The total HLW glass pour canister weight is 4200 kg and HLW glass occupies 87% of the volume. The nominal dimensions of the HLW glass pour canister are used for the calculations. The codisposal WP loaded with the HLW glass pour canisters and the canister is shown in Figure 5-7. In some calculations, the degraded HLW canisters are represented as clayey material. The composition of this clayey material is given in Table 5-8.

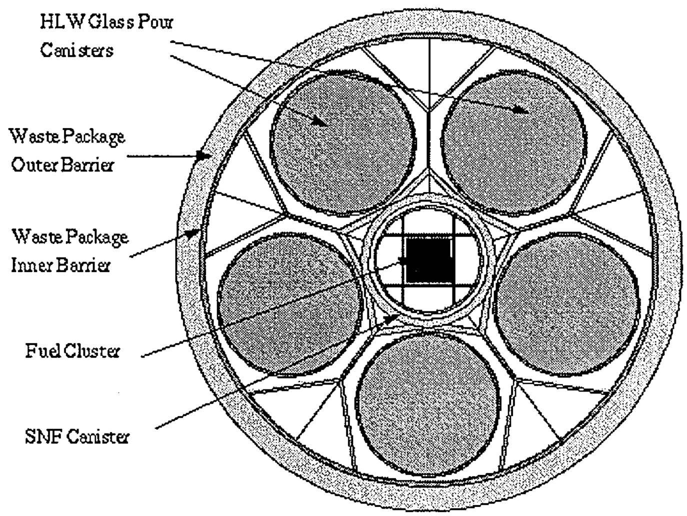

Figure 5-7. Cross-Sectional View of the Codisposal WP

5.1.5 Materials

Chemical composition of Zircaloy-4 used in the fuel cluster representation is given in Table 5-2.

Table 5-2. Chemical Composition of Zircaloy-4[a]

Element	Range (wt%)	Value Used
Fe	0.18-0.24	0.20
Cr	0.7-0.13	0.10
Fe+Cr	0.28-0.37	0.30
Sn	1.2-1.7	1.4
O	0.09-0.16	0.12
Zr	Balance	97.88

NOTE: [a] Density used: 6.56 g/cm^3.

Source: Reference 6, p. 44.

Chemical composition of Alloy 22 used for the WP inner barrier representation is given in Table 5-3.

Table 5-3. Chemical Composition of Alloy 22[a]

Element	Range (wt%)	Value Used
C	0.015 (max)	0.015
Mn	0.50 (max)	0.500
Si	0.08 (max)	0.080
Cr	20.0-22.5	21.250
Ni	54.765	54.765
Mo	12.5-14.5	13.500
Co	2.50 (max)	2.500
W	2.5-3.5	3.000
P	0.02 (max)	0.020
S	0.02 (max)	0.020
V	0.35 (max)	0.350
Fe	2.0-6.0	4.000

NOTE: [a] Density used: 8.69 g/cm^3.

Source: Reference 6, p. 30.

Chemical composition of Type 316L Stainless Steel used for canister representation is given in Table 5-4.

Table 5-4. Chemical Composition of Type 316L Stainless Steel[a]

Element	Range (wt%)	Value Used
C	0.03 (max)	0.030
Mn	2.00 (max)	2.000
P	0.045 (max)	0.045
S	0.03 (max)	0.030
Si	1.00 (max)	1.000
Cr	16.00-18.00	17.00
Ni	10.00-14.00	12.00
Mo	2.00-3.00	2.500
N	0.1 (max)	0.100
Fe	Balance	65.295

NOTE: [a] Density used: 7.98 g/cm^3.

Source: Reference 6, p. 13.

Chemical composition of A 516 Stainless Steel used for the WP representation is given in Table 5-5.

Table 5-5. Chemical Composition of A 516 Carbon Steel Grade 70 [a]

Element	Range (wt%)	Value Used
C	0.30 (max)	0.300
Mn	0.85-1.20	1.025
P	0.035 (max)	0.035
S	0.035 (max)	0.035
Si	0.15-0.40	0.275
Fe	Balance	98.33

NOTE: [a] Density used: 7.85 g/cm^3.

Source: Reference 6, p. 10.

The composition of the intact HLW glass is given in Table 5-6.

Table 5-6. Chemical Composition of HLW Glass

Element	Weight Percent	Element	Weight Percent
Li-6	9.5955E-02	Li-7	1.3804E+00
B-10	5.9176E-01	B-11	2.6189E+00
O	4.4770E+01	F	3.1852E-02
Na	8.6284E+00	Mg	8.2475E-01
Al	2.3318E+00	Si	2.1888E+01
S	1.2945E-01	K	2.9887E+00
Ca	6.6188E-01	Ti	5.9676E-01
Mn	1.5577E+00	Fe	7.3907E+00
Ni	7.3490E-01	P	1.4059E-02
Cr	8.2567E-02	Cu	1.5264E-01
Ag	5.0282E-02	Ba-137[a]	1.1267E-01
Pb	6.0961E-02	Cl	1.1591E-01
Th-232	1.8559E-01	Cs-133	4.0948E-02
Cs-135	5.1615E-03	U-234	3.2794E-04
U-236	1.0415E-03	Zn[b]	6.4636E-02
U-235	4.3514E-03	U-238	1.8666E+00
Pu-238	5.1819E-03	Pu-239	1.2412E-02
Pu-240	2.2773E-03	Pu-241	9.6857E-04
Pu-242	1.9168E-04		
Density at 25 °C = 2.85 g/cm^3 (Ref. 9, p. 2.2.1.1-4)			

NOTES: [a] Ba-138 was used in the input data for the MCNP computer code (see Assumption 3.11).
[b] Replaced by Al in the input data for the MCNP computer code (see Assumption 3.10).

Source: Reference 8, p. 7.

In Section 5.2.1.4, effect of mineral deposit from J-13 well water accumulation inside the canister is calculated. Chemical composition of this J-13 well water is given in Table 5-7.

Table 5-7. Chemical Composition of J-13 Well Water

Element	Mole Fraction	Element	Mole Fraction
O	3.33E-01	Mg	4.97E-07
Al	1.53E-10	Mn	1.83E-18
B	7.44E-08	Mo	6.00E-19
Ba	6.00E-19	N	8.50E-07
Ca	1.95E-06	Na	1.20E-05
Cl	1.21E-06	Ni	6.00E-19
Cr	6.00E-19	Np	6.00E-19
Cu	6.00E-19	Pb	6.00E-19
F	6.89E-07	Pu	6.00E-19
Fe	2.16E-14	S	1.15E-06
Gd	6.00E-19	Si	6.09E-06
H	6.67E-01	Tc	6.00E-19
C	1.26E-05	Ti	6.00E-19
P	7.57E-09	U	6.00E-19
K	7.74E-07	Zr	6.00E-19
Li	4.15E-08		

Source: Reference 11, p. 24.

In Section 5.2.1.5, effect of clay accumulation inside the canister is calculated. Prebreach clay is degraded material formed (results of the degradation of the web-like structure, the HLW glass-pour canister, and the HLW glass) prior to breach of the canister. Postbreach clay is degraded material formed after breach of canister. Chemical composition of clayey material for prebreach of the canister is presented in Table 5-8.

Table 5-8. Chemical Composition of Prebreach[a] Clay

Element	Weight Percent	Element	Weight Percent
Ag	2.8012E-02	Na	4.4497E-02
Al	1.4215E+00	Ni	1.6972E+00
Ba-137	6.8598E-02	O	3.8696E+01
Ca	3.9015E-01	P	1.6406E-02
Cl	9.2067E-03	Pb	3.7197E-02
Cr	3.5432E-02	Pu-238	1.8641E-03
Cu	7.8963E-02	Pu-239	4.4837E-03
F	3.3562E-03	Pu-240	8.2610E-04
Fe	4.1254E+01	Pu-241	3.5282E-04
H	2.6897E-01	Pu-242	7.0113E-05
K	7.2988E-02	Si	1.3590E+01
Mg	2.5330E-01	Th-232	1.1129E-01
Mn	1.5494E+00	Ti	3.6466E-01

NOTE: [a] Degraded Material at 5000 years just prior to breach of canister – Minerals Only.

Source: Reference 10, EQ6 file "N01A2204.6l".

Chemical composition of clayey material for postbreach of the canister is presented in Table 5-9. Pu and U isotopes in the clayey material were neglected because their contents were insignificant (< 0.003%).

Table 5-9. Chemical Composition of Postbreach Clay

Element	Mole Percent	Element	Mole Percent
O	56.0	P	0.0109
H	14.9	K	0.0661
Fe	15.8	Mg	0.224
Al	1.09	Mn	0.605
Ba	0.0104	Na	0.0425
Ca	0.201	Ni	0.541
Cl	0.000739	Pb	0.00373
Cu	0.0156	Si	10.3
F	0.0029	Ti	0.158
C	0.0104	Zr	0.00022

Source: Reference 11, p. 43.

5.2 DESCRIPTION

The number densities used throughout Section 5 are calculated using the following equation:

$$N = (m/V) \times N_A / M$$

where

N = the number density in atoms/cm^3
m = the mass in grams
V = the volume in cm^3
N_A= the Avogadro's number (6.02252 E+23 atoms/mole, Ref. 12, p. 933)
M = the atomic mass in grams per mole

Volumes of a cylinder segment (volume = area of the segment of a circle × length of the cylinder) are also calculated throughout Attachment III. The equation for the segment of a circle is shown below (Ref. 13, p. 125):

$$\text{Area of a Segment of a Circle} = \left(R^2 \cos^{-1}\left(\frac{R-h}{R}\right) - (R-h)\sqrt{2Rh - h^2} \right)$$

where

R = the cylinder radius
h = the height of the segment

For degradation of basket and/or canister cases, the iron content of the stainless steel is assumed to degrade into goethite, FeOOH, with a density of 4.27 g/cm^3 (Ref. 14, p. 240). The other constituents of the stainless steel are neglected and represented as water in the calculations. The codisposal WP is assumed to be fully reflected by water for all cases (see Assumption 3.5).

When goethite or clayey materials accumulate at the bottom of the canister or the WP, the coolant channel and the cruciform areas of the fuel cluster are filled with water instead of goethite and/or clay mixture. k_{eff} of the codisposal WP is larger with water instead of goethite or clay mixture in those areas as shown in Sections 6.1.3 and 6.2.2.

5.2.1 Intact Fuel Cluster

The Shippingport PWR SNF cluster is left intact for all cases outlined in this section. Figures 5-7 and 5-8 give a representation of the intact case. The fuel number density is determined by using the fuel composition data, given in Table 5-1 and the data obtained from Ref. 5. Number densities and volumes are calculated by Excel spreadsheets that are listed in Attachment III. The single C2 S2 fuel cluster in the canister with the guide plates is represented. The vacant spaces of the canister are assumed to be fully flooded with water. The canister is inside the codisposal WP, which contains five HLW glass pour canisters.

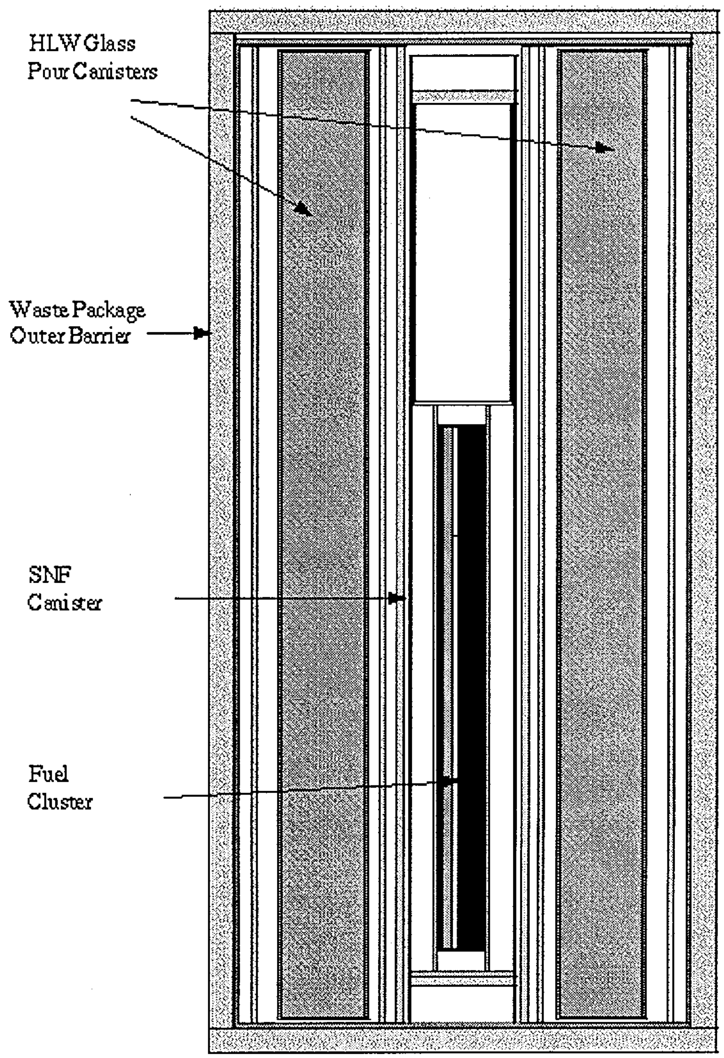

Figure 5-8. Longitudinal Cross-Sectional View of the Codisposal WP

5.2.1.1 Canister in Codisposal WP

The intact canister with the intact fuel cluster is represented in the intact codisposal WP, as shown in Figures 5-7 and 5-8. Material volumes, densities, and number densities generated for the fuel cluster are provided in Attachment III, Excel file named "sce1.number.densities.xls." k_{eff} of the intact fuel cluster is calculated based on the fuel cluster centered in the canister and the canister centered inside the WP. The canister is assumed to be fully flooded internally and reflected externally (outside of the WP) with water. The empty space outside the canister and inside the WP is represented as water. Water density is varied between 0.0 and 1.0 g/cm^3 to find the highest value of k_{eff}.

5.2.1.2 Water Intrusion into Wafer Porosity Volume and Plate Void Space

Effect of water intrusion into the plate void space is calculated. The plate void space is calculated by subtracting total fuel wafer volume from the actual fuel volume of the fuel cluster. As described in Section 5.1.1, the fuel meat occupies 87.5% of the fuel wafer volume. The remaining portion (wafer porosity volume) is void space. Effect of water intrusion into the fuel wafer porosity volume is also calculated. Water densities in the fuel wafer porosity and/or the plate void space are varied between 0.0 and 1.0 g/cm^3 to find the highest value of k_{eff}. In this scenario, the wafer porosity volume is filled with water. The same intact configuration of Figure 5-7 is used in the calculation. Material volumes, densities, and number densities generated for the fuel cluster are provided in Attachment III, Excel file named "sce2.water.in.void&porosity.xls."

5.2.1.3 Fuel Cluster in Canister with Degraded Guide Plates

The guide plates (see Figure 5-5) are represented as being completely degraded and converted into goethite. Figure 5-9 shows the cross-sectional view of the WP in this configuration. The intact fuel cluster is positioned at the bottom of the canister. The water volume fraction in the goethite is varied. All other components in the canister and codisposal WP are represented as being fully intact. The coolant and cruciform areas are filled with water. Material volumes, densities, and number densities generated for the fuel cluster and goethite are provided in Attachment III, Excel file named "sce2.basket.deg.xls."

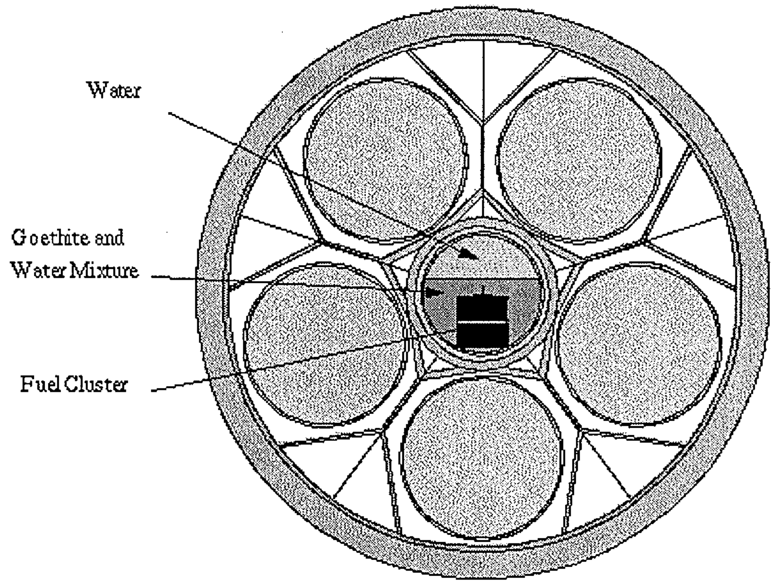

Figure 5-9. Cross-Sectional View of the Configuration with Fuel Cluster in Canister and Degraded Guide Plates

5.2.1.4 Mineral Deposit from J-13 Well Water Accumulation Inside the Canister

Effects of mineral deposit from the J-13 well water accumulation around the fuel cluster, area between plates, and the cruciform area are calculated. Figure 5-7 gives a representation of this configuration. Water around the fuel cluster, the area between plates, and the cruciform area is mixed with mineral deposit. Material volumes, densities, and number densities generated for the fuel cluster and J-13 well water are provided in Attachment III, Excel file named "sce3.j13.composition.xls."

5.2.1.5 Clay Accumulation Inside Canister

Effect of clay intrusion into the canister is calculated based on total degradation of the HLW glass pour canisters and retained integrity of the canister. The canister is positioned at the bottom of the inner barrier of the WP. Figure 5-10 shows the cross-sectional view of the WP in this configuration. Prebreach clay is degraded material prior to breach of the canister. Postbreach clay is degraded material formed after breach of the canister. The prebreach clay composition is represented outside the canister while the postbreach clay composition is used in representing clayey material inside the canister. Water inside the canister is replaced with clay. Material volumes, densities, and number densities, generated for the fuel cluster and clay are provided in Attachment III, Excel file named "sce3.clayey.new.xls." Water and clay volume fractions are varied.

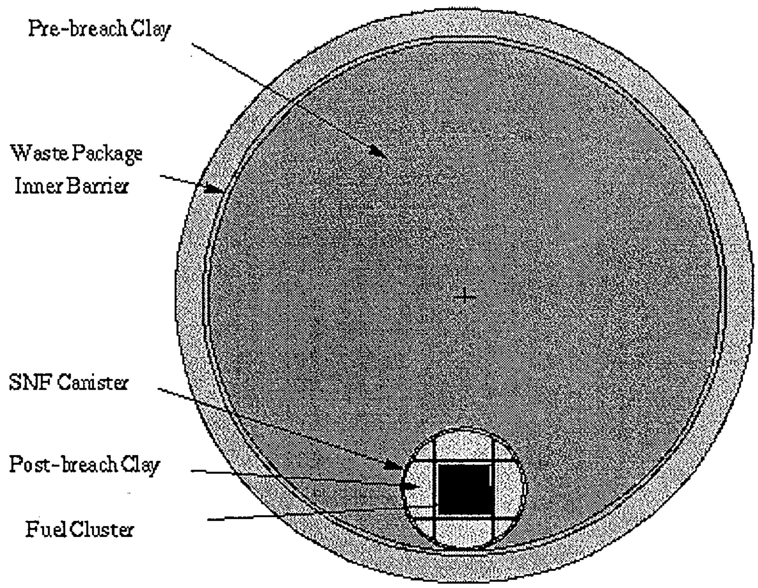

Figure 5-10. Cross-Sectional View of Clay-Accumulated Configuration

5.2.1.6 Intact Fuel Cluster with Degraded Canister and Degraded WP

In this scenario, the materials surrounding the fuel cluster degrade faster than the fuel. The canister is fully degraded and five HLW glass pour canisters are fully degraded (results of the degradation of the web-like structure, the HLW glass pour canister and HLW glass). The canister was positioned at the bottom of the inner barrier of the WP from Section 5.2.1.5, then the canister was degraded. Figure 5-11 shows the cross-sectional view of the WP in this configuration. The intact fuel cluster is surrounded by goethite (degraded canister) and clay (degraded WP, internals, HLW glass pour canisters, etc.). The goethite is mixed with clay and water with varying volume fractions. The coolant and cruciform areas are filled with water. The region above the clay, goethite, and water mixture is filled with postbreach clay. Material volumes, densities, and number densities generated for the fuel cluster, clay, and water are provided in Attachment III, Excel file named "sce6.fl.all.new.xls."

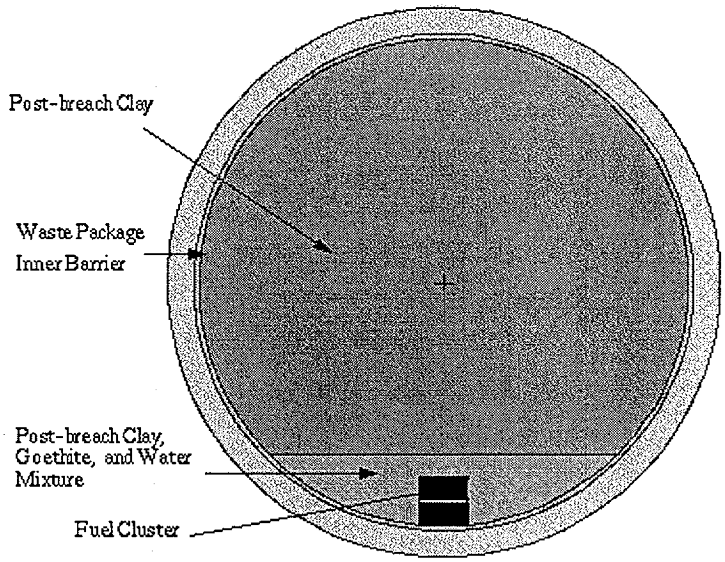

Figure 5-11. Cross-Sectional View of the Intact Fuel Cluster in the Degraded WP

5.2.2 Degraded Fuel Cluster

The Shippingport PWR SNF cluster is degraded for all cases in this section. The partially and fully degraded fuel cases are calculated. The partial degradation is represented as a fraction of fuel (UO_2-ZrO_2-CaO) leaked out of the fuel plates and homogeneously mixed with water, goethite, and/or clay. The fuel cluster is assumed to be physically intact in the partial degradation calculations. The fully degraded fuel is represented as a homogeneous mixture of UO_2, water, goethite, and clay. The degraded fuel is assumed to be chemically unchanged. The codisposal WP is assumed to be fully reflected by water for all cases. Number densities and volumes are calculated by Excel spreadsheets that are listed in Attachment III.

5.2.2.1 Partially Degraded Fuel Cluster in Canister

The fuel cluster is partially degraded and UO_2-ZrO_2-CaO is leaked out to the coolant channel and the cruciform areas as well as the central-basket area of the canister. The central-basket area is the central square area excluding the fuel cluster. The intact WP representations of Figures 5-7 and 5-8 give a representation of this partial fuel degradation case. The leaked fuel (ranging from 10 to 99% of the total fuel mass) is mixed with water in the coolant channel, the cruciform, and/or central-basket areas with varying fuel mass. The remaing portion of the fuel mass stays inside the fuel plates. Material volumes, densities, and number densities generated for the fuel leaked to the coolant area only are provided in Attachment III, Excel file named "sce4.part.cool.deg.xls." Material volumes, densities, and number densities generated for the fuel leaked to the coolant channel and the cruciform areas are provided in Attachment III, Excel file named "sce4.part.cruci.deg.xls."

5.2.2.2 Partially Degraded Fuel Cluster in Degraded Canister

The partially leaked fuel is mixed with goethite and water with varying volume fraction simulating degradation of the guide plates and the canister. Figure 5-12 gives a representation of this partial degradation case. The fuel cluster is physically intact in the representation. Material volumes, densities, and number densities generated for varying fractions of leaked fuel, goethite, and water are provided in Attachment III, Excel files, named "sce4.part10%.can.deg.xls," "sce4.part20%.can.deg.xls," "sce4.part30%.can.deg.xls," "sce4.part40%.can.deg.xls," "sce4.part50%.can.deg.xls," "sce4.part70%.can.deg.xls," and "sce4.part99%.can.deg.xls." The coolant channel and cruciform areas of the fuel cluster are filled with water instead of goethite and water mixture.

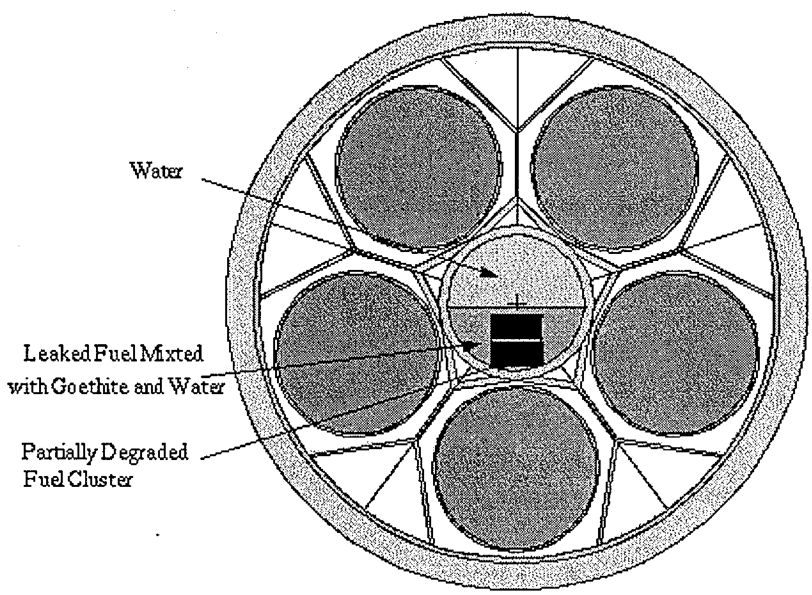

Figure 5-12. Cross-Sectional View of the Partially Degraded Fuel Cluster in the Degraded Canister

5.2.2.3 Partially Degraded Fuel Cluster with Degraded Canister and Degraded WP

In this scenario, the fuel materials and everything surrounding the fuel degrades at the same rate. The partially degraded fuel (UO_2) is mixed with degraded guide plates, degraded canister, and degraded WP (results of the degradation of the web-like structure, the HLW glass pour canister and HLW glass). Figure 5-13 gives a representation of this configuration. The fuel cluster is physically intact. The partially leaked fuel is mixed with goethite, clay, and water with varying fuel mass. Material volumes, densities and number densities generated for varying fractions of leaked fuel, goethite, and water are provided in Attachment III, Excel files named "sce5.fl.part10%.new.xls," "sce5.fl.part20%.new.xls," "sce5.fl.part30%.new.xls," "sce5.fl.part40%.new.xls," "sce5.fl.part50%.new.xls," "sce5.fl.part70%.new.xls."

Effect of spacing variation inside the cruciform area due to fuel assembly welds failure is also calculated. Material volumes, densities, and number densities generated for varying spacing of the fuel cluster are provided in Attachment III, Excel files named "sce7.0.0.new.xls," "sce7.0.24.new.xls," "sce7.0.7.new.xls," "sce7.1.0.new.xls," "sce7.1.5.new.xls," "sce7.2.0.new.xls."

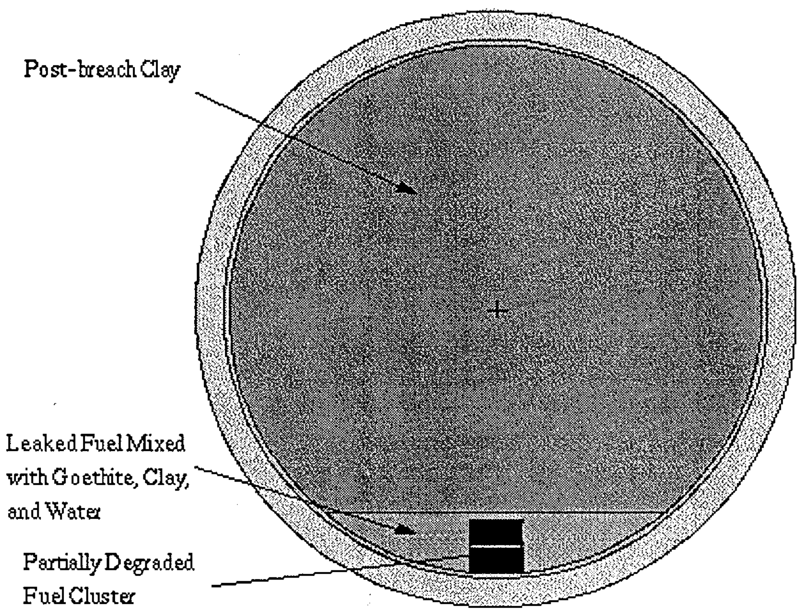

Figure 5-13. Cross-Sectional View of the Partially Degraded Fuel Cluster in the Degraded Canister

5.2.2.4 Fully Degraded Fuel in Degraded Canister and Degraded WP

The fully degraded fuel (UO_2) is mixed with goethite and clay. The degraded fuel consists of 19.5 kg of U-235, 1.423 kg of U-238, and 2.845 kg of O-16. The mixture layer of the fuel and goethite is positioned at the bottom of the inner barrier of the WP. Figure 5-14 gives a representation of this configuration. The fuel and the goethite volume fraction is varied to mix with water and clay. The postbreach clayey material occupies the non-fueled region as shown in Figure 5-14. Material volumes, densities, and number densities generated for the homogeneous mixture of fully degraded fuel, goethite, clay, and water are provided in Attachment III, Excel file named "sce8.fl.deg.xls."

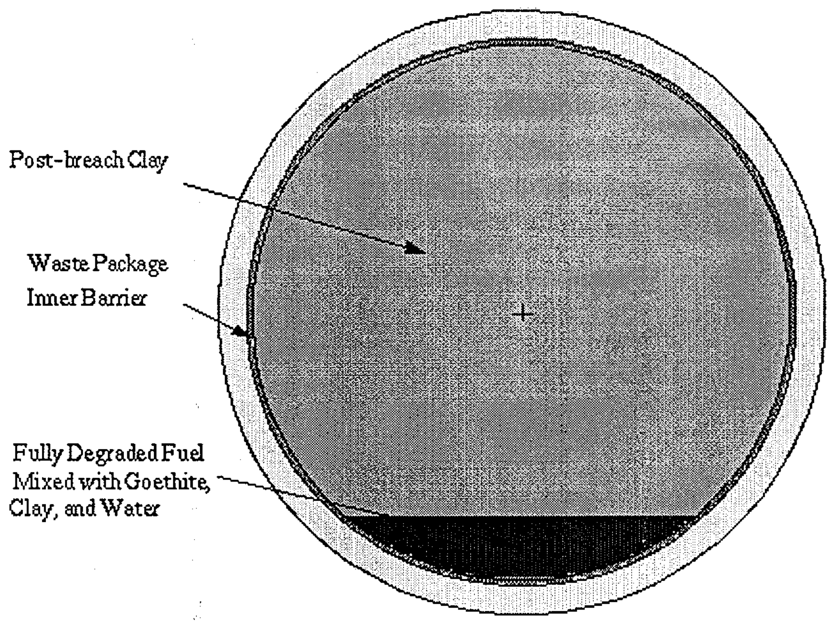

Figure 5-14. Cross-Sectional View of the Fully Degraded Fuel Cluster Configuration

6. RESULTS

MCNP results for the intact and the degraded fuel cluster are provided in this section (Tables 6-1 through 6-16). Values of k_{eff}, H/X ratio and the average energy of a neutron causing fission (AENCF) are provided. The k_{eff} value represents the average collision, absorption, and track length estimator from the MCNP calculations. The standard deviation (σ) represents the standard deviation of k_{eff} about the average combined collision, absorption, and track length estimate due to Monte Carlo calculation statistics. The H/X ratio is the number density for hydrogen divided by that for U-235 in the region containing U-235. For the intact and the partially degraded cases, the H/X atom ratio is calculated over the volume of the fuel cluster. For the fully degraded cases, the H/X atom ratio is calculated over the volume that contains the degraded fuel. The AENCF is the energy per source particle lost to fission divided by the weight per source neutron lost to fission from the "problem summary section" of the MCNP output. Also, Tables 6-1 through 6-16 contain the Excel data file names and MCNP output file names used in the calculations.

Unqualified data are used in the calculations reported in this document. Therefore, the use of any data or results from this calculation for input into documents supporting procurement, fabrication, or construction is required to be identified and controlled in accordance with appropriate procedures.

6.1 RESULTS WITH INTACT FUEL CLUSTER

6.1.1 Canister in Codisposal WP

Values of k_{eff} of the intact fuel cluster positioned at the center of the canister placed in the codisposal WP, as described in Section 5.2.1.1, are calculated. The canister is fully flooded internally and reflected externally (outside of the WP) with water. The empty space outside the canister and inside the WP is represented as water. The water density of this MCNP base case (File name: sce1.wet1) is varied between 0.0 and 1.0 g/cm^3 to find the highest value of k_{eff}. Table 6-1 summarizes MCNP results for varying water density inside the WP.

Table 6-1. Results of Intact Fuel Cluster for Varying Water Density Inside WP

Water Density (g/cm^3)	$k_{eff} \pm \sigma$	H/X Ratio	AENCF (MeV)	Excel Data File Name	MCNP Output File Name
1.0[a]	0.8415 ± 0.0011	56.7	0.0414	sce1.number.densities.xls	sce1.wet1.o
0.9	0.7948 ± 0.0010	51.0	0.0455	sce1.number.densities.xls	sce1.wet90%.o
0.8	0.7458 ± 0.0010	45.3	0.0509	sce1.number.densities.xls	sce1.wet80%.o
0.7	0.6898 ± 0.0010	39.7	0.0569	sce1.number.densities.xls	sce1.wet70%.o
0.6	0.6275 ± 0.0010	34.0	0.0654	sce1.number.densities.xls	sce1.wet60%.o
0.5	0.5626 ± 0.0010	28.3	0.0764	sce1.number.densities.xls	sce1.wet50%.o
0.4	0.4943 ± 0.0010	22.7	0.0917	sce1.number.densities.xls	sce1.wet40%.o
0.3	0.4243 ± 0.0010	17.0	0.1123	sce1.number.densities.xls	sce1.wet30%.o
0.2	0.3547 ± 0.0010	11.3	0.1439	sce1.number.densities.xls	sce1.wet20%.o
0.1	0.2714 ± 0.0010	5.7	0.2048	sce1.number.densities.xls	sce1.wet10%.o
0.0[b]	0.0934 ± 0.0002	0.0	0.6966	sce1.number.densities.xls	sce1.wet00%.o

NOTE: [a] With full reflection (reflective boundary condition) outside WP (File name sce1.wet1r.o), k_{eff} = 0.8409 ± 0.0011.
[b] Without water reflection outside the canister. With water reflection (File name: sce1.dry2), k_{eff} = 0.1640 ± 0.0010.

Water density in the cruciform area only is varied to find the largest k_{eff}. Table 6-2 summarizes MCNP results.

Table 6-2. Results of Intact Fuel Cluster for Varying Water Density in the Cruciform Area

Water Density (g/cm^3)	$k_{eff} \pm \sigma$	H/X Ratio	AENCF (MeV)	Excel Data File Name	MCNP Output File Name
1.0	0.8415 ± 0.0011	56.7	0.0414	sce1.number.densities.xls	sce1.wet1.o
0.9	0.8361 ± 0.0010	55.2	0.0422	sce1.number.densities.xls	sce1.cruci90%.o
0.8	0.8259 ± 0.0010	53.8	0.0427	sce1.number.densities.xls	sce1.cruci80%.o
0.7	0.8159 ± 0.0010	52.4	0.0438	sce1.number.densities.xls	sce1.cruci70%.o
0.6	0.8067 ± 0.0010	51.0	0.0444	sce1.number.densities.xls	sce1.cruci60%.o
0.5	0.7980 ± 0.0010	49.5	0.0453	sce1.number.densities.xls	sce1.cruci50%.o
0.4	0.7886 ± 0.0010	48.1	0.0468	sce1.number.densities.xls	sce1.cruci40%.o
0.3	0.7751 ± 0.0011	46.7	0.0473	sce1.number.densities.xls	sce1.cruci30%.o
0.2	0.7658 ± 0.0011	45.2	0.0491	sce1.number.densities.xls	sce1.cruci20%.o
0.1	0.7517 ± 0.0010	43.8	0.0506	sce1.number.densities.xls	sce1.cruci10%.o
0.0	0.7421 ± 0.0011	42.4	0.0505	sce1.number.densities.xls	sce1.cruci00%.o

6.1.2 Water Intrusion into Wafer Porosity Volume and Plate Void Space

MCNP results for water intrusion into wafer porosity volume and plate void space described in Section 5.2.1.2 are summarized in this section. The fuel meat occupies 87.5% (production density as a percentage of theoretical density) of the fuel wafer volume with the remaining portion (wafer porosity volume) filled with water. The plate void space is calculated by subtracting total fuel wafer volume from the actual fuel volume of the fuel cluster.

Table 6-3 lists the WP k_{eff} value when the full density water is introduced into just the plate void space.

Table 6-3. Results for Water Intrusion into Plate Void Space

Water Density (g/cm^3)	$k_{eff} \pm \sigma$	H/X Ratio	AENCF (MeV)	Excel Data File Name	MCNP Output File Name
1.0	0.8656 ± 0.0011	57.4	0.0395	sce2.water.in.void&porosity.xls	sce2.water.invoid1.o

Table 6-4 lists the WP k_{eff} value when the full density water is introduced into just the fuel wafer porosity volume.

Table 6-4. Results for Water Intrusion into Fuel Wafer Porosity Volume

Water Density (g/cm^3)	$k_{eff} \pm \sigma$	H/X Ratio	AENCF (MeV)	Excel Data File Name	MCNP Output File Name
1.0	0.8552 ± 0.0011	57.1	0.0399	sce2.water.in.void&porosity.xls	sce2.water.inporo1.o

Table 6-5 lists the WP k_{eff} values when the water is introduced into both fuel wafer porosity volume and plate void space. Water density in both regions are varied to find the largest k_{eff}.

Table 6-5. Results for Water Intrusion into Fuel Wafer Porosity Volume and Plate Void Space

Water Density (g/cm^3)	$k_{eff} \pm \sigma$	H/X Ratio	AENCF (MeV)	Excel Data File Name	MCNP Output File Name
1.0	0.8797 ± 0.0011	57.8	0.0387	sce2.water.in.void&porosity.xls	sce2.invoid.inporo1.o
0.9	0.8756 ± 0.0010	57.7	0.0386	sce2.water.in.void&porosity.xls	sce2.voidporo.90%.o
0.8	0.8693 ± 0.0011	57.6	0.0390	sce2.water.in.void&porosity.xls	sce2.voidporo.80%.o
0.7	0.8686 ± 0.0010	57.5	0.0392	sce2.water.in.void&porosity.xls	sce2.voidporo.70%.o
0.6	0.8622 ± 0.0010	57.4	0.0400	sce2.water.in.void&porosity.xls	sce2.voidporo.60%.o
0.5	0.8606 ± 0.0011	57.3	0.0399	sce2.water.in.void&porosity.xls	sce2.voidporo.50%.o
0.4	0.8572 ± 0.0010	57.1	0.0404	sce2.water.in.void&porosity.xls	sce2.voidporo.40%.o
0.3	0.8518 ± 0.0010	57.0	0.0410	sce2.water.in.void&porosity.xls	sce2.voidporo.30%.o
0.2	0.8497 ± 0.0010	56.9	0.0410	sce2.water.in.void&porosity.xls	sce2.voidporo.20%.o
0.1	0.8480 ± 0.0010	56.8	0.0410	sce2.water.in.void&porosity.xls	sce2.voidporo.10%.o
0.0	0.8415 ± 0.0011	56.7	0.0414	sce1.number.densities.xls	sce1.wet1.o

6.1.3 Fuel Cluster in Canister with Degraded Guide Plates

Results are given in Table 6-6 for the intact fuel cluster in the canister with degraded guide plates, as described in Section 5.2.1.3. Water volume fraction in the goethite at the bottom of the canister is varied. Water occupies the remaining portion of the canister. Result of a single case (File name: sce2.go.incluster) is provided for comparison to show that k_{eff} of the WP with water in the coolant channel and cruciform areas is more reactive than that with the goethite and water mixture. The value of k_{eff} of the WP is 0.9022 ± 0.0010 when goethite is replaced with water.

Table 6-6. Results for Fuel Cluster in Canister with Degraded Guide Plates

Goethite Volume Fraction	Water Volume Fraction	$k_{eff} \pm \sigma$	H/X Ratio	AENCF (MeV)	Excel Data File Name	MCNP Output File Name
1.0	0.0	0.8902 ± 0.0010	56.7	0.0401	sce2.basket.deg.xls	sce2.bas.100%go.o
0.8	0.2	0.8856 ± 0.0010	56.7	0.0402	sce2.basket.deg.xls	sce2.bas.80%go.o
0.6	0.4	0.8733 ± 0.0011	56.7	0.0403	sce2.basket.deg.xls	sce2.bas.60%go.o
0.6[a]	0.4	0.7063± 0.0010	6.5	0.0546	sce2.basket.deg.xls	sce2.go.incluster.o
0.4	0.6	0.8744 ± 0.0010	56.7	0.0400	sce2.basket.deg.xls	sce2.bas.40%go.o
0.23	0.77	0.8826 ± 0.0010	56.7	0.0395	sce2.basket.deg.xls	sce2.bas.23%go.o
0.0	1.0	0.9022± 0.0010	56.7	0.0376	sce2.basket.deg.xls	sce2.bas.00%go.o

NOTE: [a] Coolant and cruciform areas are filled with goethite and water mixture.

6.1.4 Mineral Deposit from J-13 Well Water Accumulation Inside the Canister

Effect of mineral deposits from J-13 well water accumulation inside the canister as described in Section 5.2.1.4 is calculated. Table 6-7 lists the WP k_{eff} values when the J-13 well water residues are introduced in different regions inside the canister. The J-13 well water is introduced in just the coolant channel and the cruciform areas in the first case. In the second case, the J-13 well water is introduced only in the area around the fuel cluster (inside the square central guide plate area) where the water acts more as a reflector. The J-13 well water inside the canister (outside the square guide plate area only) is represented in the last case.

Table 6-7. Results for Mineral Deposit from J-13 Well Water Accumulation Inside the Canister

Case	$k_{eff} \pm \sigma$	H/X Ratio	AENCF (MeV)	Excel Data File Name	MCNP Output File Name
J-13 Well Water in Coolant and Cruciform Regions	0.8424 ± 0.0010	56.7	0.0417	sce3.j13.composition.xls	sce3.j13.cool.cruci.o
J-13 Well Water around Fuel Cluster	0.8426 ± 0.0011	56.7	0.0415	sce3.j13.composition.xls	sce3.j13.inbas.o
J-13 Well Water in DOE SNF Canister	0.8437 ± 0.0010	56.7	0.0413	sce3.j13.composition.xls	sce3.j13.incan.o

6.1.5 Clay Accumulation Inside the Canister

Results are presented in Table 6-8 for clay accumulation inside the canister as described in Section 5.2.1.5. Clay volume fraction in water is varied.

Table 6-8. Results for Clay Accumulation Inside the Canister

Clay Volume Fraction	Water Volume Fraction	$k_{eff} \pm \sigma$	H/X Ratio	AENCF (MeV)	Excel Data File Name	MCNP Output File Name
0.0	1.0	0.8409 ± 0.0010	56.7	0.0413	sce3.clayey.new.xls	sce3.tcly0.o
0.1	0.9	0.8113 ± 0.0010	52.3	0.0440	sce3.clayey.new.xls	sce3.tcly10%.o
0.3	0.7	0.7488 ± 0.0011	43.5	0.0510	sce3.clayey.new.xls	sce3.tcly30%.o
0.5	0.5	0.6817 ± 0.0009	34.6	0.0593	sce3.clayey.new.xls	sce3.tcly50%.o
0.7	0.3	0.6115 ± 0.0009	25.8	0.0707	sce3.clayey.new.xls	sce3.tcly70%.o

6.1.6 Intact Fuel Cluster with Degraded Canister and Degraded WP

The intact fuel cluster is surrounded by a mixture of the degraded canister and the degraded WP materials, as described in Section 5.2.1.6. The goethite is mixed with clay and water with varying volume fractions. The region above the clay, goethite, and water mixture is filled with postbreach clayey material. The results are presented in Table 6-9.

Table 6-9. Results for Intact Fuel Cluster with Degraded Canister and Degraded WP

Goethite Fraction	Clay Fraction	Water Fraction	$k_{eff} \pm \sigma$	H/X Ratio[a]	AENCF (MeV)	Excel Data File Name	MCNP Output File Name
1.0[b]	0.0	0.0	0.9058 ± 0.0010	56.7	0.0403	sce6.fl.all.new.xls	sce6.100%go.claytop.o
1.0[c]	0.0	0.0	0.8883 ± 0.0011	56.7	0.0407	sce6.fl.all.new.xls	sce6.100%go.watop.o
0.9	0.05	0.05	0.9034 ± 0.0010	56.7	0.0403	sce6.fl.all.new.xls	sce6.90%go.5%clay.o
0.7	0.00	0.3	0.9011 ± 0.0010	56.7	0.0400	sce6.fl.all.new.xls	sce6.70%go.0%clay.o
0.7	0.15	0.15	0.9039 ± 0.0011	56.7	0.0404	sce6.fl.all.new.xls	sce6.70%go.15%clay.o
0.7	0.30	0.0	0.9108 ± 0.0010	56.7	0.0405	sce6.fl.all.new.xls	sce6.70%go.30%clay.o
0.5	0.25	0.25	0.8999 ± 0.0011	56.7	0.0404	sce6.fl.all.new.xls	sce6.50%go.25%clay.o
0.3	0.35	0.35	0.8876 ± 0.0011	56.7	0.0408	sce6.fl.all.new.xls	sce6.30%go.35%clay.o
0.1	0.45	0.45	0.8881 ± 0.0010	56.7	0.0402	sce6.fl.all.new.xls	sce6.10%go.45%clay.o
0.0	1.0	0.0	0.9198 ± 0.0011	56.7	0.0405	sce6.fl.all.new.xls	sce6.0%go.100%clay.o
0.0	0.0	1.0	0.9067 ± 0.0010	56.7	0.0379	sce6.fl.all.new.xls	sce6.0%go.0%clay.o

NOTES: [a] constant inside fuel cluster
[b] region above goethite filled with clay
[c] region above goethite filled with water

6.2 RESULTS WITH DEGRADED FUEL CLUSTER

6.2.1 Partially Degraded Fuel Cluster in the Intact Canister

The fuel cluster is partially degraded and the fuel is leaked out to the coolant channels and the cruciform areas as well as the central-basket area of the canister as described in Section 5.2.2.1. The central-basket area is the central square area excluding the fuel cluster. Table 6-10 lists the WP k_{eff} value for 10% fuel leakage into the coolant channel area only. Table 6-11 lists the WP k_{eff} value for 10% fuel leakage into the coolant channel and cruciform areas.

Table 6-10. Results for Partially Leaked Fuel in Coolant Channels

Fuel Leakage Fraction	$K_{eff} \pm \sigma$	H/X Ratio	AENCF (MeV)	Excel Data File Name	MCNP Output File Name
0.1	0.8438 ± 0.0011	60.4	0.0408	sce4.part.cool.deg.xls	sce4.fpd.10%.cool1.o

Table 6-11. Results for Partially Leaked Fuel in Coolant Channel and Cruciform Areas

Fuel Leakage Fraction	$k_{eff} \pm \sigma$	H/X Ratio	AENCF (MeV)	Excel Data File Name	MCNP Output File Name
0.1	0.8603 ± 0.0011	60.4	0.0387	sce4.part.cruci.deg.xls	sce4.fpd.10%.cruci.o

The WP k_{eff} value for the 10% fuel leakage into the coolant channel, cruciform, and central-basket areas is also calculated as shown in Table 6-12. It is observed that the 10% fuel leakage to the coolant channel, cruciform, and the central-basket areas results in the larger k_{eff} compared to the leakage to the coolant channel only, or to the coolant channel and the cruciform areas. Because of this largest k_{eff} change, the 10% leak case in Table 6-12 was selected and the leakage fraction of the fuel to these areas was increased to find the largest k_{eff}. Table 6-12 summarizes MCNP results.

Table 6-12. Results for Partially Leaked Fuel Redistributed in Coolant Channel, Cruciform, and Central-Basket Areas

Fuel Leakage Fraction	$k_{eff} \pm \sigma$	H/X Ratio	AENCF (MeV)	Excel Data File Name	MCNP Output File Name
0.1	0.8714 ± 0.0011	60.9	0.0362	sce4.part.inbas.deg.xls	sce4.fpd.10%.inbas.o
0.3	0.9055 ± 0.0010	72.9	0.0297	sce4.part.inbas.deg.xls	sce4.fpd.30%.inbas.o
0.5	0.9206 ± 0.0011	94.1	0.0258	sce4.part.inbas.deg.xls	sce4.fpd.50%.inbas.o
0.6	0.9252 ± 0.0010	103.8	0.0249	sce4.part.inbas.deg.xls	sce4.fpd.60%.inbas.o
0.7	0.9230 ± 0.0011	141.0	0.0253	sce4.part.inbas.deg.xls	sce4.fpd.70%.inbas.o
0.8	0.9280 ± 0.0010	154.0	0.0246	sce4.part.inbas.deg.xls	sce4.fpd.80%.inbas.o
0.99	0.9241 ± 0.0011	309.3	0.0252	Sce4.part.inbas.deg.xls	sce4.fpd.99%.inbas.o

6.2.2 Partially Degraded Fuel Cluster in Degraded Canister

The partially leaked fuel is mixed with degraded canister as described in Section 5.2.2.2. The leaked UO_2 is mixed with goethite with varying water volume fraction. Table 6-13 lists the WP k_{eff} values.

Table 6-13. Results for Partially Degraded Fuel Cluster in Degraded Canister

Fuel Leakage Fraction	Fuel and Goethite Volume Fraction	Water Volume Fraction	$k_{eff} \pm \sigma$	H/X Ratio	AENCF (MeV)	Excel Data File Name	MCNP Output File Name
0.1	1.0	0.0	0.9079 ± 0.0010	63.0	0.0353	sce4.part10%.can.deg.xls	sce4.fpd.10%.candeg.o
0.2	1.0	0.0	0.9140 ± 0.0010	70.9	0.0305	sce4.part20%.can.deg.xls	sce4.fpd.20%.candeg.o
0.3	1.0	0.0	0.9149 ± 0.0010	81.0	0.0260	sce4.part30%.can.deg.xls	sce4.fpd.30%.candeg.o
0.4	1.0	0.0	0.9168 ± 0.0010	94.5	0.0223	sce4.part40%.can.deg.xls	sce4.fpd.40%.candeg.o
0.4	0.8	0.2	0.9230 ± 0.0010	94.5	0.0206	sce4.part40%.can.deg.xls	sce4.0.8.40%.candeg.o
0.4	0.8	0.2	0.7273 ± 0.0010	82.2	0.0278	sce4.part40%.can.deg.xls	sce4.0.8.40%.sen.o[a]
0.4	0.6	0.4	0.9234 ± 0.0010	94.5	0.0200	sce4.part40%.can.deg.xls	sce4.0.6.40%.candeg.o
0.4	0.4	0.6	0.9112 ± 0.0011	94.5	0.0197	sce4.part40%.can.deg.xls	sce4.0.4.40%.candeg.o
0.5	1.0	0.0	0.9121 ± 0.0010	113.4	0.0192	sce4.part50%.can.deg.xls	sce4.fpd.50%.candeg.o
0.7	1.0	0.0	0.8663 ± 0.0010	188.9	0.0131	sce4.part70%.can.deg.xls	sce4.fpd.70%.candeg.o
0.99	1.0	0.0	0.7141 ± 0.0010	566.8	0.0128	sce4.part99%.can.deg.xls	sce4.fpd.99%.candeg.o

NOTE: [a] This case has a mixture of leaked fuel, goethite, and water in the coolant and cruciform control rod channel areas. Other cases in the table have water in these areas.

Result of a case (sce4.0.8.40%.sen) is provided to show that k_{eff} of the WP with water in the coolant and cruciform control rod channel areas is larger than that with the mixture of leaked fuel, goethite, and water.

6.2.3 Partially Degraded Fuel Cluster in Degraded Canister and Degraded WP

The partially degraded fuel is mixed with goethite, clay, and water as described in Section 5.2.2.3. The goethite and the clay fractions are varied. The remaining volume is filled with water. Table 6-14 lists the WP k_{eff} values for varying fractions of leaked fuel, goethite, and the clayey material.

Table 6-14. Results for Partially Degraded Fuel Cluster in Degraded Canister and Degraded WP

Fuel Leakage Fraction	Goethite Fraction	Clay Fraction	$k_{eff} \pm \sigma$	H/X Ratio	AENCF (MeV)	Excel Data File Name	MCNP Output File Name
0.1	0.9	0.05	0.9092 ± 0.0011	63.0	0.0348	sce5.fl.part10%.new.xls	sce5.fl.10%leak.5%clay.o
0.2	0.9	0.05	0.9121 ± 0.0011	70.9	0.0297	sce5.fl.part20%.new.xls	sce5.fl.20%leak.5%clay.o
0.3	0.9	0.05	0.9170 ± 0.0012	81.0	0.0256	sce5.fl.part30%.new.xls	sce5.fl.30%leak.5%clay.o
0.4	0.9	0.05	0.9147 ± 0.0010	94.5	0.0220	sce5.fl.part40%.new.xls	sce5.fl.40%leak.5%clay.o
0.4	0.7	0.15	0.9016 ± 0.0010	94.5	0.0225	sce5.fl.part40%.new.xls	sce5.40%leak.70%go.o
0.4	0.5	0.25	0.8909 ± 0.0011	94.5	0.0224	sce5.fl.part40%.new.xls	sce5.40%leak.50%go.o
0.4	0.3	0.35	0.8686 ± 0.0010	94.5	0.0234	sce5.fl.part40%.new.xls	sce5.40%leak.30%go.o
0.4	0.1	0.45	0.8323 ± 0.0012	94.5	0.0256	sce5.fl.part40%.new.xls	sce5.40%leak.10%go.o
0.5	0.9	0.05	0.9105 ± 0.0010	113.4	0.0185	sce5.fl.part50%.new.xls	sce5.fl.50%leak.5%clay.o
0.7	0.9	0.05	0.8821 ± 0.0010	188.9	0.0127	sce5.fl.part70%.new.xls	sce5.fl.70%leak.5%clay.o

Effect of subcluster spacing change inside the cruciform area due to fuel assembly welds failure as described in Section 5.2.2.3 is also calculated. The third case of Table 6-9 (MCNP file name: sce6.90%go.5%clay) was used as a basis for spacing change. In this case, the mixture outside the fuel cluster contains 90% goethite, 5% clay, and 5% water. Table 6-15 summarizes the WP k_{eff} for varying spacing between the fuel subclusters.

Table 6-15. Results for Cruciform Area Spacing Variation of Degraded Fuel Cluster in Degraded Canister and Degraded WP

Spacing Between Fuel Subclusters (cm)	Goethite Fraction	Clay Fraction	$k_{eff} \pm \sigma$	H/X Ratio	AENCF (MeV)	Excel Data File	MCNP Output File Name
5.08	0.9	0.05	0.7713 ± 0.0011	109.8	0.0389	sce7.2.0.new.xls	sce7.2.0.90%go.5%clay.o
3.81	0.9	0.05	0.8416 ± 0.0010	91.3	0.0373	sce7.1.5.new.xls	sce7.1.5.90%go.5%clay.o
2.54	0.9	0.05	0.8927 ± 0.0010	73.9	0.0371	sce7.1.0.new.xls	sce7.1.0.90%go.5%clay.o
1.78	0.9	0.05	0.9066 ± 0.0010	64.0	0.0386	sce7.0.7.new.xls	sce7.0.7.90%go.5%clay.o
1.19[a]	0.9	0.05	0.9034 ± 0.0010	56.7	0.0403	sce6.fl.all.new.xls	sce6.90%go.5%clay.o
0.61	0.9	0.05	0.8802 ± 0.0011	49.5	0.0438	sce7.0.24.new.xls	sce7.0.24.90%go.5%clay.o
0.01	0.9	0.05	0.8406 ± 0.0012	42.5	0.0489	sce7.0.0.new.xls	sce7.0.0.90%go.5%clay.o

NOTE: [a] corresponds to intact spacing of 0.47 inch.

6.2.4 Fully Degraded Fuel in Degraded Canister and Degraded WP

The fully degraded fuel (19.5 kg of U-235, 1.423 kg of U-238, and 2.845 kg of O-16) is homogeneously mixed with goethite, clay, and water as described in Section 5.2.2.4. The goethite and the clay fractions are varied. The remaining volume is filled with water. Table Table 6-16 lists the WP k_{eff} values for varying fractions of goethite and the clayey material.

Table 6-16. Results for Fully Degraded Fuel in Degraded Canister and Degraded WP

Goethite Fraction	Clay Fraction	Water Fraction	$k_{eff} \pm \sigma$	H/X Ratio	AENCF (MeV)	Excel Data File	MCNP Output File Name
1.0	0.00	0.0	0.8423 ± 0.0020	188.9	0.0125	sce8.fl.deg.new.xls	sce8.100%go.o
0.9	0.05	0.05	0.7251± 0.0016	220.2	0.0124	sce8.fl.deg.new.xls	sce8.fl.90%go.5%clay.o
0.7	0.15	0.15	0.7266 ± 0.0020	305.6	0.00946	sce8.fl.deg.new.xls	sce8.fl.70%go.15%clay.o
0.5	0.25	0.25	0.7082 ± 0.0018	459.4	0.00800	sce8.fl.deg.new.xls	sce8.fl.50%go.25%clay.o
0.3	0.35	0.35	0.6263 ± 0.0014	818.2	0.00511	sce8.fl.deg.new.xls	sce8.fl.30%go.35%clay.o
0.1	0.45	0.45	0.3538 ± 0.0010	2612.5	0.00330	sce8.fl.deg.new.xls	sce8.fl.10%go.45%clay.o

7. ATTACHMENTS

Attachment I: Shippingport PWR Single-Assembly DOE SNF Basket Assembly (Sketch No.: SK-0125 REV 00)

Attachment II: List of MCNP output files provided on electronic media (compact disk [CD]) (Ref. 15).

Attachment III: List of Excel spreadsheet files provided on electronic media (CD) (Ref. 15).

Attachment IV: Document Input Reference Sheets.

8. REFERENCES

1. Briesmeister, J.F., ed. 1997. *MCNP- A General Monte Carlo N-Particle Transport Code.* LA-12625-M, Version 4B. Los Alamos, New Mexico: Los Alamos National Laboratory (LANL). ACC: MOL.19980624.0328.

2. Paxton, H.C. and Pruvost, N.L. 1987. *Critical Dimensions of Systems Containing U-235, Pu-239 and U-233, 1986 Revision.* LA-10860-MS. Los Alamos, New Mexico: LANL. TIC: 209447.

3. Atherton, R.; Kikta, E.J.; and Sherman, J., eds. 1968. *PWR Core 2 Reactor Design Description Report.* WAPD-296. Pittsburgh, Pennsylvania: Bettis Atomic Power Laboratory. TIC: 243596.

4. Civilian Radioactive Waste Management System (CRWMS) Management and Operating (M&O) Contractor 1998. *Software Qualification Report for MCNP Version 4B2, A General Monte Carlo N-Particle Transport Code.* CSCI: 30033 V4B2LV. DI: 30033-2003 Rev. 01. Las Vegas, Nevada: CRWMS M&O. ACC: MOL.19980622.0637.

5. DOE (U.S. Department of Energy) 1999. *Shippingport PWR (HEU Oxide) Fuel Characteristics for Disposal Criticality Analysis.* DOE/SNF/REP-040, Revision 0. Washington, D.C.: U.S. Department of Energy, Office of Spent Fuel Management and Special Projects. TIC: 243528.

6. CRWMS M&O 1999. *Waste Package Materials Properties.* BBA000000-01717-0210-00017 REV 00. Las Vegas, Nevada: CRWMS M&O. ACC: MOL.19990407.0172.

7. DOE (U.S. Department of Energy) 1998. *Preliminary Design Specification for Department of Energy Standardized Spent Nuclear Fuel Canisters, Volume 1 - Design Specification.* DOE/SNF/REP-011, Revision 1. Washington, D.C.: U.S. Department of Energy, Office of Spent Fuel Management and Special Projects. TIC: 241528.

8. CRWMS M&O 1999. *DOE SRS HLW Glass Chemical Composition.* BBA000000-01717-0210-00038 REV 00. Las Vegas, Nevada: CRWMS M&O. ACC: MOL.19990215.0397.

9. Stout, R.B. and Leider, H.R., eds. 1991. *Preliminary Waste Form Characteristics Report.* Version 1.0. Livermore, California: Lawrence Livermore National Laboratory. ACC: MOL.19940726.0118.

10. CRWMS M&O 1999. *Electronic Media for EQ6 Calculations for Chemical Degradation of Enrico Fermi Spent Nuclear Fuel Waste Packages.* BBA000000-01717-0210-00029 Revision 00. Las Vegas, Nevada: CRWMS M&O. ACC: MOL.19990507.0237.

11. CRWMS M&O 1999. *EQ6 Calculation for Chemical Degradation of Shippingport PWR (HEU Oxide) Spent Nuclear Fuel Waste Package.* CAL-EDC-MD-000002 REV 00. Las Vegas, Nevada: CRWMS M&O. ACC: MOL.19991220.0322.

12. Benedict, M.; Pigford, T.H.; and Levi, H.W. 1981. *Nuclear Chemical Engineering.* Second Edition. New York, New York: McGraw-Hill Book Company. TIC: 245089.

13. Beyer, W.H., ed.1987. *CRC Standard Mathematical Tables.* 28th Edition. Boca Raton, Florida: CRC Press. TIC: 240507.

14. Roberts, W.L.; Rapp, G.R., Jr.; and Weber, J. 1974. *Encyclopedia of Minerals.* Pages 172, 240, 241, 413, 500, 689, 690. New York, New York: Van Nostrand Reinhold Co. TIC: 238571.

15. CRWMS M&O 1999. *Electronic Media (CD) for Intact and Degraded Criticality Calculations for the Codisposal of Shippingport PWR Fuel in a Waste Package, CAL-EDC-NU-000002 REV 00.* Las Vegas, Nevada: CRWMS M&O. ACC: MOL.19991217.0162.

16. Walker, F.W.; Parrington, J.R.; and Feiner, F. 1989. *Nuclides and Isotopes, Fourteenth Edition: Chart of the Nuclides.* San Jose, California: General Electric Company. TIC: 201637.

Attachment I

Shippingport PWR Single-Assembly DOE SNF Basket Assembly

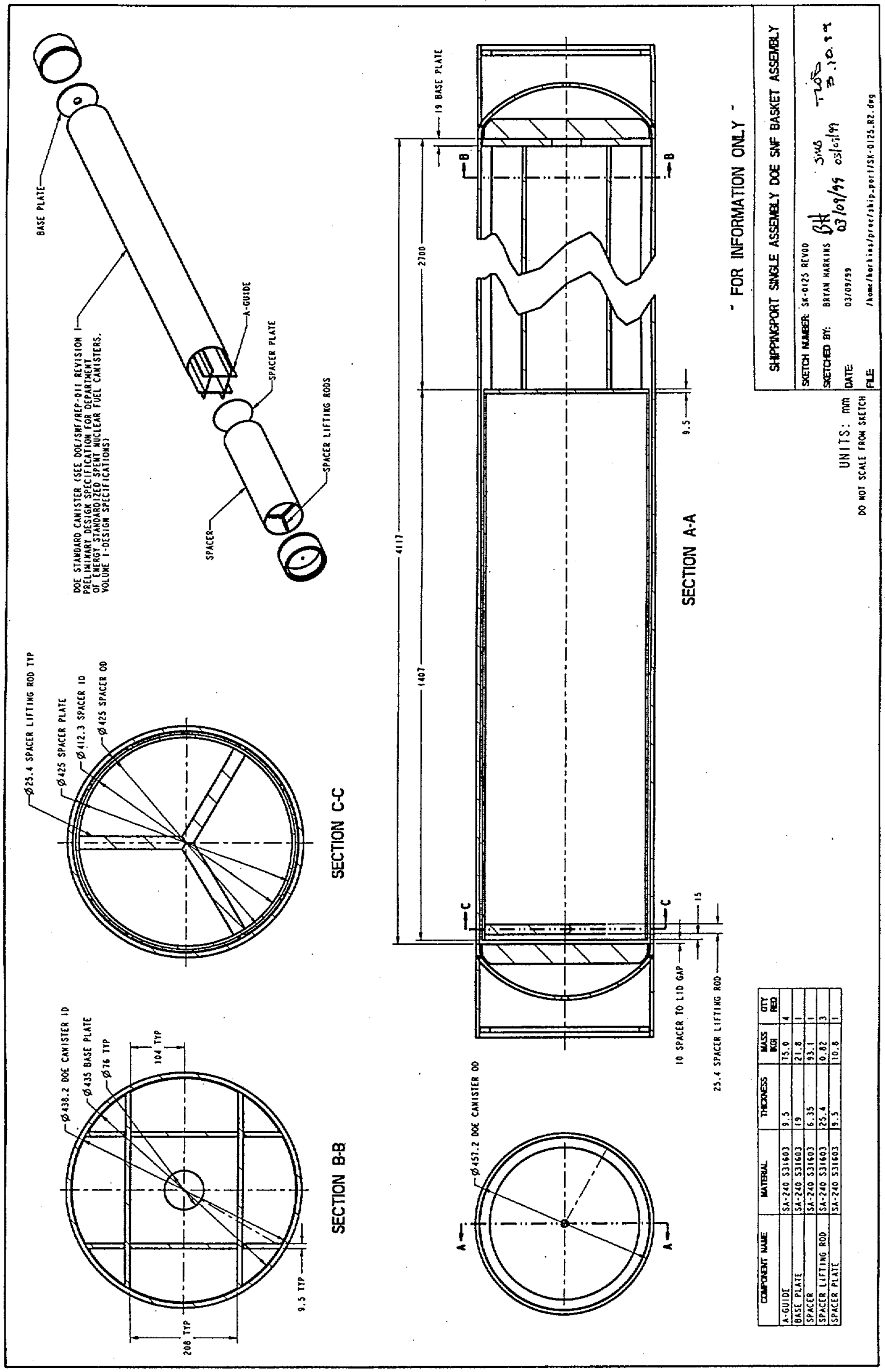

COMPONENT NAME	MATERIAL	THICKNESS	MASS (KG)	QTY REQ
A-GUIDE	SA-240 S31603	9.5	75.0	4
BASE PLATE	SA-240 S31603	19	21.8	1
SPACER	SA-240 S31603	6.35	93.1	1
SPACER LIFTING ROD	SA-240 S31603	25.4	0.82	3
SPACER PLATE	SA-240 S31603	9.5	10.8	1

Attachment II

Table II-1. MCNP Output Files Contained on the Electronic Media (Ref. 15)

Bytes Used	Date Last Accessed	File name	Table Used
899,898	7/15/99	sce1.wet1.o	Table 6-1
908,721	12/17/99	sce1.wet1r.o	Table 6-1
893,674	7/16/99	sce1.dry2.o	Table 6-1
899,504	7/15/99	sce1.wet30%.o	Table 6-1
899,434	7/15/99	sce1.wet60%.o	Table 6-1
900,158	7/15/99	sce1.wet90%.o	Table 6-1
895,833	7/16/99	sce1.wet00%.o	Table 6-1
950,099	7/16/99	sce1.wet10%.o	Table 6-1
899,504	7/16/99	sce1.wet40%.o	Table 6-1
899,847	7/16/99	sce1.wet70%.o	Table 6-1
899,816	7/16/99	sce1.wet20%.o	Table 6-1
899,816	7/17/99	sce1.wet50%.o	Table 6-1
900,064	7/17/99	sce1.wet80%.o	Table 6-1
900,565	7/15/99	sce1.cruci20%.o	Table 6-2
900,684	7/15/99	sce1.cruci50%.o	Table 6-2
900,881	7/16/99	sce1.cruci80%.o	Table 6-2
900,741	7/16/99	sce1.cruci00%.o	Table 6-2
900,762	7/17/99	sce1.cruci40%.o	Table 6-2
900,570	7/16/99	sce1.cruci30%.o	Table 6-2
900,689	7/17/99	sce1.cruci60%.o	Table 6-2
900,881	7/17/99	sce1.cruci90%.o	Table 6-2
900,666	7/17/99	sce1.cruci10%.o	Table 6-2
900,762	7/18/99	sce1.cruci70%.o	Table 6-2
918,256	7/15/99	sce4.fpd.30%.inbas.o	Table 6-12
918,323	7/16/99	sce4.fpd.60%.inbas.o	Table 6-12
918,141	7/16/99	sce4.fpd.80%.inbas.o	Table 6-12
918,893	7/17/99	sce4.fpd.10%.inbas.o	Table 6-12
918,187	7/17/99	sce4.fpd.50%.inbas.o	Table 6-12
918,398	7/17/99	sce4.fpd.70%.inbas.o	Table 6-12
917,829	7/17/99	sce4.fpd.99%.inbas.o	Table 6-12
911,987	7/15/99	sce2.water.invoid1.o	Table 6-3
912,641	7/15/99	sce2.water.inporo1.o	Table 6-4
910,883	7/15/99	sce2.voidporo.30%.o	Table 6-5
911,080	7/17/99	sce2.voidporo.50%.o	Table 6-5

911,136	7/16/99	sce2.voidporo.70%.o	Table 6-5
910,858	7/19/99	sce2.voidporo.60%.o	Table 6-5
911,026	7/16/99	sce2.invoid.inporo1.o	Table 6-5
911,179	7/16/99	sce2.voidporo.40%.o	Table 6-5
910,969	7/17/99	sce2.voidporo.80%.o	Table 6-5
911,176	7/17/99	sce2.voidporo.10%.o	Table 6-5
910,860	7/17/99	sce2.voidporo.90%.o	Table 6-5
911,405	7/18/99	sce2.voidporo.20%.o	Table 6-5
1,121,787	7/15/99	sce2.bas.100%go.o	Table 6-6
896,269	7/15/99	sce2.bas.40%go.o	Table 6-6
976,258	7/15/99	sce2.bas.80%go.o	Table 6-6
955,387	7/15/99	sce2.bas.00%go.o	Table 6-6
939,144	7/15/99	sce2.bas.23%go.o	Table 6-6
896,457	7/16/99	sce2.bas.60%go.o	Table 6-6
942,125	7/16/99	sce2.go.incluster.o	Table 6-6
854,838	7/26/99	sce7.0.0.90%go.5%clay.o	Table 6-15
831,110	7/20/99	sce7.0.7.90%go.5%clay.o	Table 6-15
863,510	7/20/99	sce7.1.5.90%go.5%clay.o	Table 6-15
831,228	7/20/99	sce7.0.24.90%go.5%clay.o	Table 6-15
831,226	7/20/99	sce7.1.0.90%go.5%clay.o	Table 6-15
935,351	7/20/99	sce7.2.0.90%go.5%clay.o	Table 6-15
911,052	7/15/99	sce3.j13.inbas.o	Table 6-7
939,807	7/16/99	sce3.j13.cool.cruci.o	Table 6-7
912,688	7/17/99	sce3.j13.incan.o	Table 6-7
934,484	11/5/99	sce3.tcly10%.o	Table 6-8
933,695	11/5/99	sce3.tcly70%.o	Table 6-8
934,437	11/5/99	sce3.tcly30%.o	Table 6-8
883,971	11/5/99	sce3.tcly0.o	Table 6-8
933,811	11/5/99	sce3.tcly50%.o	Table 6-8
1,084,461	7/20/99	sce6.10%go.45%clay.o	Table 6-9
860,028	7/20/99	sce6.70%go.0%clay.o	Table 6-9
841,528	7/22/99	sce6.90%go.5%clay.o	Table 6-9
988,432	7/20/99	sce6.100%go.claytop.o	Table 6-9
1,135,481	7/23/99	sce6.clay.inclust.o	Table 6-9
925,243	7/20/99	sce6.70%go.15%clay.o	Table 6-9
817,426	7/21/99	sce6.100%go.watop.o	Table 6-9
895,439	7/22/99	sce6.50%go.25%clay.o	Table 6-9
954,970	7/21/99	sce6.70%go.30%clay.o	Table 6-9
909,425	7/22/99	sce6.30%go.35%clay.o	Table 6-9

853,873	7/23/99	sce6.0%go.100%clay.o	Table 6-9
840,254	7/23/99	sce6.0%go.0%clay.o	Table 6-9
915,797	7/15/99	sce4.fpd.10%.cool1.o	Table 6-10
915,081	7/15/99	sce4.fpd.10%.cruci.o	Table 6-11
1,031,991	7/15/99	sce4.0.8.40%.sen.o	Table 6-13
976,986	7/16/99	sce4.fpd.40%.candeg.o	Table 6-13
913,479	7/16/99	sce4.0.4.40%.candeg.o	Table 6-13
1,011,070	7/16/99	sce4.fpd.10%.candeg.o	Table 6-13
1,087,441	7/16/99	sce4.fpd.50%.candeg.o	Table 6-13
892,205	7/16/99	sce4.0.6.40%.candeg.o	Table 6-13
1,101,578	7/16/99	sce4.fpd.20%.candeg.o	Table 6-13
1,085,284	7/17/99	sce4.fpd.70%.candeg.o	Table 6-13
1,057,934	7/17/99	sce4.0.8.40%.candeg.o	Table 6-13
970,852	7/17/99	sce4.fpd.30%.candeg.o	Table 6-13
846,194	7/17/99	sce4.fpd.99%.candeg.o	Table 6-13
858,893	7/20/99	sce5.40%leak.50%go.o	Table 6-14
879,612	7/20/99	sce5.fl.20%leak.5%clay.o	Table 6-14
870,585	7/20/99	sce5.fl.50%leak.5%clay.o	Table 6-14
881,023	7/20/99	sce5.40%leak.10%go.o	Table 6-14
859,802	7/20/99	sce5.40%leak.70%go.o	Table 6-14
838,374	7/20/99	sce5.fl.30%leak.5%clay.o	Table 6-14
876,497	7/21/99	sce5.fl.70%leak.5%clay.o	Table 6-14
837,065	7/21/99	sce5.40%leak.30%go.o	Table 6-14
928,125	7/22/99	sce5.fl.10%leak.5%clay.o	Table 6-14
879,401	7/22/99	sce5.fl.40%leak.5%clay.o	Table 6-14
182,371	7/20/99	sce8.100%go.o	Table 6-16
187,014	7/20/99	sce8.90%go.5%clay.o	Table 6-16
187,067	7/20/99	sce8.30%go.35%clay.o	Table 6-16
187,110	7/20/99	sce8.50%go.25%clay.o	Table 6-16
187,422	7/20/99	sce8.10%go.45%clay.o	Table 6-16
187,030	7/20/99	Sce8.70%go.15%clay.o	Table 6-16

Attachment III

Table III-1. Excel Spreadsheet Files Contained on the Electronic Media (Ref. 15)

File Name	Description	Tables Used
sce1.number.densities.xls	Calculated Number Densities for Intact Shippingport PWR Fuel	Tables 6-1, 6-2
sce2.water.in.void&porosity.xls	Calculated Number Densities for Water Intrusion in Wafer Porosity Volume and Plate Void Space of the Shippingport PWR Fuel	Tables 6-3, 6-4, 6-5
sce2.basket.deg.xls	Calculated Number Densities for Degraded Guide Plates	Table 6-6
sce3.j13.composition.xls	Calculated Number Densities for J-13 Well Water Accumulation inside the DOE SNF Canister	Table 6-7
sce3.clayey.new.xls	Calculated Number Densities for Postbreach Clay Accumulation inside the DOE SNF Canister	Table 6-8
sce6.fl.all.new.xls	Calculated Number Densities for Postbreach Clay mixed with Degraded DOE SNF Canister	Table 6-9
sce4.part.cool.deg.xls	Calculated Number Densities for Fuel Leakage into the Coolant Channel	Table 6-10
sce4.part.cruci.deg.xls	Calculated Number Densities for Fuel Leakage into the Coolant Channel and Cruciform Areas	Table 6-11
sce4.part.inbas.deg.xls	Calculated Number Densities for Fuel Leakage into the Coolant Channel, Cruciform, and Central-Basket Areas	Table 6-12
sce4.part10%.can.deg.xls	Calculated Number Densities for 10% Fuel Leakage into the Degraded DOE SNF Canister	Table 6-13
sce4.part20%.can.deg.xls	Calculated Number Densities for 20% Fuel Leakage into the Degraded DOE SNF Canister	Table 6-13
sce4.part30%.can.deg.xls	Calculated Number Densities for 30% Fuel Leakage into the Degraded DOE SNF Canister	Table 6-13
sce4.part40%.can.deg.xls	Calculated Number Densities for 40% Fuel Leakage into the Degraded DOE SNF Canister	Table 6-13
sce4.part50%.can.deg.xls	Calculated Number Densities for 50% Fuel Leakage into the Degraded DOE SNF Canister	Table 6-13
sce4.part70%.can.deg.xls	Calculated Number Densities for 70% Fuel Leakage into the Degraded DOE SNF Canister	Table 6-13
sce4.part99%.can.deg.xls	Calculated Number Densities for 99% Fuel Leakage into the Degraded DOE SNF Canister	Table 6-13
sce5.fl.part10%.new.xls	Calculated Number Densities for 10% Fuel Leakage into the Degraded DOE SNF Canister Mixed with Postbreach Clayey Material	Table 6-14
sce5.fl.part20%.new.xls	Calculated Number Densities for 20% Fuel Leakage into the Degraded DOE SNF Canister Mixed with Postbreach Clayey Material	Table 6-14
sce5.fl.part30%.new.xls	Calculated Number Densities for 30% Fuel Leakage into the Degraded DOE SNF Canister Mixed with Postbreach Clayey Material	Table 6-14
sce5.fl.part40%.new.xls	Calculated Number Densities for 40% Fuel Leakage into the Degraded DOE SNF Canister Mixed with Postbreach Clayey Material	Table 6-14
sce5.fl.part50%.new.xls	Calculated Number Densities for 50% Fuel Leakage into the Degraded DOE SNF Canister Mixed with Postbreach Clayey Material	Table 6-14
sce5.fl.part70%.new.xls	Calculated Number Densities for 70% Fuel Leakage into the Degraded DOE SNF Canister Mixed with Postbreach Clayey Material	Table 6-14

sce7.2.0.new.xls	Calculated Number Densities for 2.0-inch Spacing between Fuel Subclusters	Table 6-15
sce7.1.5.new.xls	Calculated Number Densities for 1.5-inch Spacing between Fuel Subclusters	Table 6-15
sce7.1.0.new.xls	Calculated Number Densities for 1.0-inch Spacing between Fuel Subclusters	Table 6-15
sce7.0.7.new.xls	Calculated Number Densities for 0.7-inch Spacing between Fuel Subclusters	Table 6-15
sce7.0.24.new.xls	Calculated Number Densities for 0.24-inch Spacing between Fuel Subclusters	Table 6-15
sce7.0.0.new.xls	Calculated Number Densities for 0.01-inch Spacing between Fuel Subclusters	Table 6-15
sce8.fl.deg.new.xls	Calculated Number Densities for Fully Degraded Fuel Mixed with the Degraded DOE SNF Canister and Postbreach Clayey Material	Table 6-16

OFFICE OF CIVILIAN RADIOACTIVE WASTE MANAGEMENT

DOCUMENT INPUT REFERENCE SHEET

1. Document Identifier No./Rev.:	Change:	Title:
CAL-EDC-NU-000002 REV 00	N/A	Intact and Degraded Criticality Calculations for the Codisposal of Shippingport PWR Fuel in a Waste Package

Input Document							8. TBV Due To		
2. Technical Product Input Source Title and Identifier(s) with Version		3. Section	4. Input Status	5. Section Used in	6. Input Description	7. TBV/TBD Priority	Unqual.	From Uncontrolled Source	Un-confirmed
2a 1	Briesmeister, J.F., ed. 1997. *MCNP-A General Monte Carlo N-Particle Transport Code.* LA-12625-M, Version 4B. Los Alamos, New Mexico: Los Alamos National Laboratory. ACC: MOL.19980624.0328.	Entire	N/A	2, 4, 6	Computer code used for keff calculations	N/A	N/A	N/A	N/A
2	Paxton, H.C. and Pruvost, N.L. 1987. *Critical Dimensions of Systems Containing U-235, Pu-239 and U-233, 1986 Revision.* LA-10860-MS. Los Alamos, New Mexico: Los Alamos National Laboratory. TIC: 209447.	p. 107, Fig. 45	N/A	3	Effective infinite water reflection	N/A	N/A	N/A	N/A
3	Atherton, R.; Kikta, E.J.; and Sherman J., eds. 1968. *PWR Core 2 Reactor Design Description Report.* WAPD-296. Pittsburgh, Pennsylvania: Bettis Atomic Power Laboratory. TIC: 243596.	p. 22	N/A	3	Density of fuel	N/A	N/A	N/A	N/A

OFFICE OF CIVILIAN RADIOACTIVE WASTE MANAGEMENT
DOCUMENT INPUT REFERENCE SHEET

1. Document Identifier No./Rev.:	Change:	Title:
CAL-EDC-NU-000002 REV 00	N/A	Intact and Degraded Criticality Calculations for the Codisposal of Shippingport PWR Fuel in a Waste Package

Input Document			4. Input Status	5. Section Used in	6. Input Description	7. TBV/TBD Priority	8. TBV Due To		
2. Technical Product Input Source Title and Identifier(s) with Version		3. Section					Unqual.	From Uncontrolled Source	Un-confirmed
2a 4	CRWMS M&O 1998. *Software Qualification Report for MCNP Version 4B2 A General Monte Carlo N-Particle Transport Code. CSCI: 30033 V4B2LV.* DI: 30033-2003, Rev. 01. Las Vegas, Nevada: CRWMS M&O. ACC: MOL.19980622.0637.	Entire	N/A	2, 4	Qualification report for MCNP	N/A	N/A	N/A	N/A
5	DOE (U.S. Department of Energy) 1999. *Shippingport PWR Fuel Characteristics for Disposal Criticality Analysis.* DOE/SNF/REP-040, Revision 0. Washington, D.C.: U.S. Department of Energy, Environmental Management, Spent Fuel Management Office. TIC: 243528.	Entire	N/A	3, 5	Input parameters for Shippingport PWR fuel	N/A	N/A	N/A	N/A
6	CRWMS M&O 1999. *Waste Package Materials Properties.* BBA000000-01717-0210-00017 REV 00. Las Vegas, Nevada: CRWMS M&O. ACC: MOL.19990407.0172.	p. 10, 13, 30, 44.	N/A	5	Material compositions of Alloy 22, 316L SS, A 516 Carbon Steel, Zr-4	N/A	N/A	N/A	N/A

OFFICE OF CIVILIAN RADIOACTIVE WASTE MANAGEMENT
DOCUMENT INPUT REFERENCE SHEET

1. Document Identifier No./Rev.:	Change:	Title:
CAL-EDC-NU-000002 REV 00	N/A	Intact and Degraded Criticality Calculations for the Codisposal of Shippingport PWR Fuel in a Waste Package

Input Document							8. TBV Due To		
	2. Technical Product Input Source Title and Identifier(s) with Version	3. Section	4. Input Status	5. Section Used in	6. Input Description	7. TBV/TBD Priority	Unqual.	From Uncontrolled Source	Un-confirmed
2a 7	DOE (U.S. Department of Energy) 1998. *Preliminary Design Specification for Department of Energy Standardized Spent Nuclear Fuel Canisters, Volume I - Design Specification.* DOE/SNF/REP-011, Revision 1. Washington, D.C.: U.S. Department of Energy, Office of Spent Fuel Management and Special Projects. TIC: 241528	Entire	N/A	5	DOE SNF canister dimensions and materials.	N/A	N/A	N/A	N/A
8	CRWMS M&O 1999. *DOE SRS HLW Glass Chemical Composition.* BBA000000-01717-0210-00038 REV 00. Las Vegas, Nevada: CRWMS M&O. ACC: MOL.19990215.0397.	p.7	TBV-3145	5	Chemical composition of HLW glass. This reference uses existing preliminary data from "*Preliminary Waste Form Characteristics Report*" ACC: MOL.19940726.0118	3	✓	N/A	N/A
9	Stout, R.B. and Leider, H.R., eds. 1991. *Preliminary Waste Form Characteristics Report.* Version 1.0. Livermore, California: Lawrence Livermore National Laboratory. ACC: MOL.19940726.0118	p. 2.2.1.1-4	TBV-3152	5	Density of HLW glass.	3	✓	N/A	N/A

OFFICE OF CIVILIAN RADIOACTIVE WASTE MANAGEMENT
DOCUMENT INPUT REFERENCE SHEET

1. Document Identifier No./Rev.:	Change:	Title:
CAL-EDC-NU-000002 REV 00	N/A	Intact and Degraded Criticality Calculations for the Codisposal of Shippingport PWR Fuel in a Waste Package

Input Document							8. TBV Due To			
	2. Technical Product Input Source Title and Identifier(s) with Version	3. Section	4. Input Status	5. Section Used in	6. Input Description	7. TBV/TBD Priority	Unqual.	From Uncontrolled Source	Un-confirmed
2a 10	CRWMS M&O 1999. *EQ6 Calculations for Chemical Degradation of Enrico Fermi Spent Nuclear Fuel Waste Packages.* BBA000000-01717-0210-00029 REV 00. Las Vegas, Nevada: CRWMS M&O. ACC: MOL.19990702.0030.	Entire	TBV-3178	5	Basis for composition of pre-breach clayey material.	3	✓	N/A	N/A
11	CRWMS M&O 1999. *EQ6 Calculation for Chemical Degradation of Shippingport PWR (HEU Oxide) Spent Nuclear Fuel Waste Packages.* CAL-EDC-MD-000002 REV 00. Las Vegas, Nevada: CRWMS M&O. ACC: MOL.19991220.0322.	p. 24 p. 43	TBV-3179 TBV-3180	5 5	Material composition of J-13 well water Basis for composition of post-breach clayey material	3 3	✓ ✓	N/A N/A	N/A N/A
12	Benedict, M.; Pigford, T.H.; and Levi, H.W. 1981. *Nuclear Chemical Engineering, Second Edition.* New York, New York: McGraw-Hill Book Company. TIC: 245089.	p. 22	N/A	5	Avogadro's number	N/A	N/A	N/A	N/A

OFFICE OF CIVILIAN RADIOACTIVE WASTE MANAGEMENT

DOCUMENT INPUT REFERENCE SHEET

1. Document Identifier No./Rev.:	Change:	Title:
CAL-EDC-NU-000002 REV 00	N/A	Intact and Degraded Criticality Calculations for the Codisposal of Shippingport PWR Fuel in a Waste Package

Input Document			4. Input Status	5. Section Used in	6. Input Description	7. TBV/TBD Priority	8. TBV Due To		
	2. Technical Product Input Source Title and Identifier(s) with Version	3. Section					Unqual.	From Uncontrolled Source	Un-confirmed
13	Beyer, W.H., ed. 1987. *CRC Standard Mathematical Tables.* 28th Edition. Boca Raton, Florida: CRC Press. TIC: 240507.	p. 125	N/A	5	Area of a segment of a circle	N/A	N/A	N/A	N/A
14	Roberts, W.L.; Rapp, G.R., Jr.; and Weber, J. 1974. *Encyclopedia of Minerals*. Pages 172, 240, 241, 413, 500, 689, 690. New York, New York: Van Nostrand Reinhold Company. TIC: 238571.	p. 240	N/A	5	Density of FeOOH	N/A	N/A	N/A	N/A
15	CRWMS M&O 1999. *Electronic Media (CD-ROM); Intact and Degraded Criticality Calculations for the Codisposal of Shippingport PWR Fuel in a Waste Package, CAL-EDC-NU-000002 REV 00.* Las Vegas, Nevada: CRWMS M&O. ACC: MOL.19991117.0093	Entire	N/A	6	MCNP output files and Excel data files	N/A	N/A	N/A	N/A
16	Walker, F.W.; Parrington, J.R.; Feiner, F. 1989. *Nuclides and Isotopes, Fourteenth Edition: Chart of the Nuclides.* San Jose, California: General Electric Company. TIC: 201637.	p. 8	N/A	3	Capture cross sections and resonance integrals for Zn, Al, Ba-137, and Ba-138	N/A	N/A	N/A	N/A